DOE/ID/13236--2

DEVELOPMENT OF LEAD-FREE COPPER ALLOY GRAPHITE CASTINGS

Annual Report for the Period January through December 1995

P. K. Rohatgi

October 1996

Work Performed Under Contract No. FC07-94ID13236

For
U.S. Department of Energy
Assistant Secretary for
Energy Efficiency and Renewable Energy
Washington, DC

By
University of Wisconsin-Milwaukee

DISCLAIMER

DOE/ID/13236--2
(DE97050521)
Distribution Category UC-1420

DEVELOPMENT OF LEAD-FREE COPPER ALLOY GRAPHITE CASTINGS

Annual Report for the Period January through December 1995

By
P. K. Rohatgi

October 1996

Work Performed Under Contract No. DE-FC07-93ID13236

Prepared for
U.S. Department of Energy
Assistant Secretary for
Energy Efficiency and Renewable Energy
Washington, D.C.

Prepared by
University of Wisconsin-Milwaukee
Milwaukee, WI 53201

DISCLAIMER

This technical report was prepared as an account of work sponsored by an agency of the United States Government. Neither the United States Government nor any agency thereof, nor any of their employees, makes any warranty, express, or limited or assumes any legal liability or responsibility of the accuracy, completeness, or usefulness of any information, apparatus, product, or process disclosed, or represents that its use would not infringe privately owned rights. References herein to any specific commercial product, process, or service by trade name, trademark, manufacturer, or otherwise, do not necessarily constitute or imply its endorsement, recommendation, or favoring by the United States Government or any agency thereof. The views and opinions of authors expressed herein do not necessarily state or reflect those of the United States Government or ant agency thereof.

ABSTRACT

The distribution of graphite particles in graphite containing copper alloy was further improved very significantly using several procedures and technological modifications. The developed techniques attacked the graphite distribution problem in two ways. Realizing that clustering of very fine (5um) graphite particles is one of the two major problems, a pretreatment process has been developed using aluminum powders to deagglomerate graphite particles. Along with this, a two-stage stirring technique was used to first incorporate and then to distribute uniformly the deagglomerated particles in the melt.

During this year, based on these developments, several components were cast to evaluate the castability of Cu alloy-graphite melts. In addition, machinability tests were done to clearly established that addition of graphite particles improve the machinability of copper MMC alloys over and above that of monolithic copper alloys. The results show that the machining chip sizes and cutting forces of Cu alloys containing graphite particles are smaller than these of the corresponding monolithic Cu alloys. This clearly establishes that the presence of graphite particles in copper alloy improves the machinability in a fashion similar to lead additions to copper alloys.

Centrifugal casting of shapes of different sizes appear to be a very attractive method for casting graphite containing copper alloys, since all the graphite particles (regardless of their distribution in the melt) are forced to segregate to the inner periphery of the castings where they impart a very desirable solid lubrication property for bushing and bearing use. A very large number of cylindrical elements of lead bearing copper alloys are now used for similar bearing bushing applications and the manufacturers of these type of bearings are under safety and health hazard pressure to remove lead. These manufacturers have expressed a great deal of interest in this DOE sponsored work at UWM. This year several parameters for centrifugal casting of copper graphite alloys have been established. Since graphite particles decrease melt viscosity, a

relatively higher melt temperature may be required to provide the required fluidity. However, at the higher temperature, some zinc may be lost. Therefore, additional studies are under way to develop a proper technology for centrifugal casting of Cu alloy-graphite castings.

Triboblogy test were done for cylindrically cast C90300 copper alloy samples containing 13 vol% graphite particles. Teh resut shows that as the load increases, the weight loss of the pin increases, and then at a higher load it decreases. As the load increases, the contact surface is increasingly deformed due to the applied load, and with traction caused by the friction force the deformed asperities are broken and removed as wear particles, leading to weight loss of the pins. It is to be noted that the weight loss of the disk increases with increasing load and it is less than the pin wear.

TABLE OF CONTENTS

LIST OF FIGURES

LIST OF TABLES

1. Introduction

This report summarizes the work undertaken by UWM Foundry and Composite Laboratories under DOE project entitled "Development of Lead-Free Copper Alloy-Graphite Castings". As a continuation of first year's work (1994), machinability testing, centrifugal casting, tribology, evaluation of selected shaped castings such as plumbing components, and mold evaluation studies were pursued. In addition, based on the earlier report which indicated that prior agglomeration of graphite particles in the melt may cause problems to obtaining a proper graphite distribution, studies to improve the distribution of graphite were continued with the development of several modified techniques.

The earlier results showed that the graphite particles are usually agglomerated in clumps of sizes a hundred times larger than the individual size of the graphite particles (about 5 um). To reduce the agglomeration of the graphite particles, the graphite powder was intimately mixed with aluminum powder and added to the melt. The microstructure observations show that this pretreatment helped in significantly breaking up the clumps of graphite particles, resulting in a dispersal of fine particles in the melt, and in the casting. Obviously, the floatation velocity of the clumps of graphite particles decreased significantly by this pretreatment because their size becomes much smaller and Stoke's law predicts the velocity to decrease as the square of the particle diameter. This pretreatment may also help to reduce the use of titanium as a wetting agent and thus avoid additional chemical reaction product formation on the particles.

The machinability tests were conducted to determine the effect of graphite on the machinability of Cu alloy. The sizes of the chips from Cu alloys containing the graphite particles were found to be smaller than those from the base Cu alloy, this demonstrates that the presence of graphite particles in the matrix reduces the chip size and this is one of the criteria indicating improvement in the machinability of Cu alloy. This work suggests

that graphite can be a substitute for lead which is primarily added to improve the machinability of copper alloys.

Centrifugal casting of Cu alloy containing graphite particles established the feasibility of making hollow cylindrical castings, in which the higher graphite particles are segregated to the inner periphery making them ideally suited for bearing applications. Currently, a large number of copper alloy bearings containing lead are manufactured and there is pressure to remove the lead which provides lubrication. The graphite particles will provide lubrication and, therefore, can replace lead.

Tribological work done at UWM, shows that the presence of graphite particles at the inner periphery of the centrifugally cast copper alloys provides excellent tribological properties. Three leading bearing industries, includeing Glacier Clevite, Bunting Bearing and Federal Mogul, express their interest in our ongoing project on Lead-Free Copper alloys and requested us for samples of our Pb free Cu alloys for their in house testing.

2. Scope of Tasks

In the second year of the program, primary efforts were directed towards:

1. Distribution of graphite particles in the casting

2. Optimization of centrifugal casting

3. Characterization of structure and properties of centrifugal castings.

4. Determination of tribological properties.

3. Technical Works

3.1 Technical Background

3.1.1 Distribution of graphite particles in the casting

In the initial technology development, the distribution and recovery of graphite particles were improved using a suitable stirrer design, combined with a two-stage stirring technique. However, some large clusters of graphite particles still persisted. In the as-received condition, fine graphite particles(5-10um) are always present in clusters of hundreds of particles caused by triboelectricity during their production. Even though graphite particles are heated to reduce their moisture content, the short range electrostatic forces acting between the fine particles do not fully dissipate even under intense shearing action of melt stirring. The residual agglomerated clusters of graphite particles in the melt during mixing enhance their buoyancy effect and floatation takes place at a much faster rate causing an undesirable non-uniform distribution. On the other hand, even when a good distribution of graphite particles is obtained in a casting, there is always a small reaction to form titanium carbide from titanium used as wetting agent. The titanium carbide formed on the graphite particle has high hardness which should be minimized to obtain high machinability. On the basis of continuing microstructural evaluation, we had suggested earlier that to obtaining copper-graphite components a small amount of aluminum powder may be added. Aluminum powder density matches the graphite density, intensive premixing of graphite and aluminum particles prior to addition in the melt largely dissipates the short range forces holding the fine graphite particles in large clusters. Under this condition, this wetting action will be enhanced and lesser Ti may have to be added.

To obtain the desired goals of very uniform fine graphite distribution in the casting with the minimum use of titanium as the wetting agent, the different technological conditions must be both necessary and sufficient. Declustering of graphite particles is

necessary, but not sufficient. So further effort was directed to modify the technology of the mode of addition of the particles into the melt. Instead of additions of rather disorganized lose particles as practiced heretofore in the two stage stirring technique, the graphite particles premixed with Al and Ti particles in a preset proportion were added very gradually in a more organized and compact form through a specially developed opening in the furnace cover. Additional technology modification was directed to the replacement of Al with Cu particles and modification of stirrer design to minimize vortex formation and to establish uniformity of distribution. Because graphite distribution uniformity is the key to the success of graphite casting production and its control and repeatability at the foundry level, continuing effort is directed to its further development.

3.1.2 Centrifugal casting of copper-graphite composite.

Centrifugal casting technology is a well established industrial process which produces castings weighing from a few ounces to several tons in diverse ferrous, non-ferrous and high temperature alloys. However, commercial application of centrifugal casting technology, so far, has been limited to monolithic alloys with the exception of gray cast iron which is a MMC made of iron and graphite particles.

The centrifugal rotational speed imparted to the molten alloy composite subject the particulate in the melt to gravitational accelerations many times that of one 'g' (9.81 m/s^2) encountered in gravity castings. The higher force provides unique opportunities for selective distribution and concentration of the composite particles at the desired locations. For example, a light particle such as graphite in copper alloy melt moves inward and generates an excellent tribological surface with a very strong backing of copper alloy without any graphite in it. On the other hand, an aluminum alloy with SiC particles when centrifugally cast will develop into a cylinder having a lightweight but an abrasion resistant outside surface due to preferential movement and concentration SiC on the outside matrix. Combination of selected particles of different densities, shape and size as

well as intrinsic alloy having different properties, with particles dispersed in the matrix alloys of suitable chemistry can be centrifugally cast to provide highly tailor-made inside and outside surfaces having a combination of unique properties.

The distribution of graphite particles in casting and the thickness of graphite rich zone depend on many factors such as the amount of graphite incorporated, the rotational speed of the mold, the mold material and its heat transfer properties, and the superheat of the melt. Specially, since the graphite particle has a lubrication property, the concentration of graphite provides unique tribological property to the copper alloy which by itself exhibits very poor frictional behavior. To obtain a proper casting, the relationship between each factor must be identified. On the other hand, since copper alloy has a high solidification rate, and the addition of graphite to the copper melt reduces the melt temperature and thus reducing melt viscosity, a proper technique is necessary to obtain cylindrical copper-graphite alloy castings.

3.1.3 Tribological properties of Cu alloy containing graphite

The surface of solids are rough. During contact between the two solid surfaces, interaction takes place highly locally between the two surface asperities. When the load is applied to the two surfaces in contact, the number of asperity contacts increases. During rubbing, a material is usually significantly altered by the friction forces compared to their initial conditions. Friction and wear occur. They depend on the properties of the two solid bodies such as hardness, solubility, thermal conductivity, Young's modulus and an external conditions such as applied load and velocity, and environmental conditions.

The friction between two solid surfaces generates heat. That causes solid body to be weakened and/or change their phases. The surface layer is deformed elastically as well as plastically. Strain produced in the surface layer may lead to chemical and mechanical changes. As a result of frictional heating the contact temperature may exceed the recovery temperature, the surface layer may become soft and ductile. In addition, the surface layer

becomes smoother. These changes in the surface layer of metals during sliding are dependent on the temperature gradient produced, which leads to a gradient in the mechanical properties and to enhanced diffusion processes. The temperature gradient in the bulk material results in establishing a residual stress in the surface layer when the bulk material cools down.

The 60 Cu/40 Zn brass is a good tribological martial. A typical plot of wear loss of brass pins shows a run-in stage followed by a steady state wear. Wear rate of brass pin sliding on steel bush as a function of load shows a linearity up to this transition load of 8 kg at speed 59cm/s. When the load is greater than the transition load, a gross deformation of the subsurface of the pin occurs, and then the layer becomes brittle. It is important to know the transition load because beyond the transition load severe wear occurs.

Graphite is widely known as a solid lubricant elements due to its layered structure. The presence of graphite particles in the surface layer of a copper alloy reduces friction and wear. Therefore, Cu alloy containing graphite particles can be applications in bearings. Literature shows that as the content of graphite in Cu alloy increases, the frictional coefficient and wear decreases, because the presence of graphite at the asperity contact areas reduces the total contact area between copper alloy metal-to-metal asperity surfaces. The continuous supply of graphite particles may be a major factor to obtain a good tribological property. In addition, the presence of graphite in the surface layer may affect heat transfer which affects the hardness and other strength properties of the surface layer.

3.1.4 Machinabiblity of Lead Free Copper Graphite Alloys

One of major considerations in the development of copper alloy-graphite composites to replace leaded copper alloys used in plumbing components is that the metal matrix composite must have a similar machinability rating to that of the alloy it is to replace. Machinability tests on metals and alloys are conducted through one or more of several simple machine operations, for example, single-point lathe turning, drilling, and

milling. Several criteria commonly used for rating machinability are volume removal rate, degree of tool wear, power requirements, machined chip length, machined surface roughness, and temperature increment and vibration generation during machining. In our study, lathe and drilling tests were conducted for machinability evaluation of the composites.

3.2 Experimental Results and Discussion

3.2.1 Distribution of graphite particles

A critical evaluation of the as-received graphite powder shows a non-homogeneous distribution of particles in the bulk powder which consists of different sizes of agglomerates as well as loose individual particles. It has been shown experimentally that the agglomerates of these fine particles are highly stable, and mixing by stirring them in molten metal can not fully breakup the agglomerates into their component individual particles. During production of graphite particles, rubbing and sliding between particles cause the generation of triboelectricity, a form of static electrical charge that builds up on the particle surface. These charges may remain on the surface which is very large for 5 um size particles. To develop the technology of improving the distribution of graphite particles in the castings, the graphite particles were mixed with aluminum powder, and then the agglomeration of graphite particles was evaluated.

To obtain deagglomerated powder, it was decided to intensively mix aluminum powder with the as-received graphite powder. Fig. 1 shows schematically the sieve blending techniques tried with graphite and a model powder resin. Figs. 2, 3 and 4 show the mixed graphite-resin particle distribution following the preparation techniques shown in Figs. 1 a, b and c, respectively. It may be noted that the addition of resin powder with graphite particles improves the distribution of graphite particles. A mixture of graphite particles (5 um, density = 2.3g/cm^3) and aluminum powder (10 um, density = 2.8 g/cm^3) was obtained with intensive shaking in a glass container. This blended powder (Al: Gr 1:2 by wt) was used for the casting of yellow brass graphite composites with titanium as the wetting agent. Typical microstructures of composites are shown in Fig. 5. Figs. 5(a) and (b) clearly show that premixing with aluminum powder has broken up the graphite agglomerates into individual graphite particles and they are distributed more uniformly in the matrix alloy. The results confirmed our prediction that the proposed

procedure helps to obtain composites with much more uniform distribution of the graphite phase and will significantly decrease the tendency of floatation. Microstructure observation shows that the above effect of aluminum powder remains effective though aluminum dissolves rapidly in copper alloy melt. Even after 1 hour at a temperature 950 C, the size of agglomerate is about 50 um as compared to the much larger agglomerates (800 um) obtained using the graphite powder in the as-received condition without mixing them with aluminum powder. According the stok'es law, the flotation velocity of the particle is a function of the square of the particle size. Therefore, an increase in the particle size 10 times increases the floatation velocity 100 times. Because of the high alloying tendency of aluminum in copper melt, the aluminum-graphite mixture added to copper has no tendency to form an agglomerate of their own. Only on rare occasions, because of some possible non-uniformity in temperature distribution, particles of undissolved aluminum were observed in the matrix. The deagglomerated graphite particles will also float at a much lower rate in the copper alloy melt than the agglomerated particles.

A successful development of copper alloy-graphite composites and production of high quality parts requires that the fine particles of graphite become uniformly distributed by stirring in the molten copper alloy matrix. Earlier, we have conducted investigations on microstructures of a number of copper components, quantity of wetting agent and chemical composition of the copper alloy matrix. It was noted that in all cases, the as-received graphite particles have a strong tendency to form large agglomerates and retain that in the melt. The number of agglomerates as well as their size increases from the bottom to the top part of the ingot, where agglomerates as large as 800 um were observed consisting of thousands of 5um individual particles. We note that the finer graphite particles mixed with aluminum powder helps in improving wettability between the copper melt and the graphite particle, and reduces the floatation velocity.

3.2.2 Machinability of copper-graphite composite

The major advantage of leaded brass is that the presence of lead in copper alloy matrix provides a good machinability. In this test, the effect of graphite on machinability on copper alloy was evaluated since the addition of graphite in copper alloy may improve the machinability due to its softness and lubricity. Lathe turning and drilling tests were conducted for machinability evaluation.

Lathe test: Samples for machinability test were cast using an induction furnace. The graphite particles preheated to 200C in an oven were added into the melt at 1150C using stir casting technique. Both 60/40 brass and brass-1.5wt % graphite composite were cast using three inch long and one inch diameter steel mold for lathe turning tests. The samples were machined with a standard C3 carbide insert, and cutting and feed force data were obtained using a three-component dynamometer and Labview software at Tufts University. All samples were machined at 840 rpm at three different feed rates of 0.005, 0.010, and 0.016 in/rev and three different depths of cut of 0.020, 0.060, and 0.100 inch. Chips were collected after each run, inspected, and photographed.

Table 1 shows the force data collected for some of the runs for one inch diameter brass alloy and brass-graphite composite. Fig. 6 shows cutting force as a function of feed rate and depth of cut at a cutting speed of 660 sfpm for one inch diameter brass and brass-graphite composite. Fig. 6 shows that cutting force increases with increasing feed rate and depth of cut for both brass and brass-graphite composite. Notably, brass with graphite requires less than half the cutting force required for monolithic brass at all feed rates and depths of cut.

Table 2 shows the feed force data for brass and brass-graphite composite. Fig. 7 shows the feed forces as a function of the depth of cut and feed rate. It is noted that as feed rate and depth of cut increase, feed forces increase: also the presence of graphite

reduces feed forces. Specially, it is obvious that at the higher feed rate brass-graphite composite reduces feed forces very dramatically when compared with monolithic brass.

Tables 3 and 4 show machinability force data for 3 inch diameter brass and brass-graphite composite castings. Figs. 8 and 9 show that cutting forces increase with increasing feed rate and depth of cut, and the cutting force for brass-graphite composite is lower than that of brass. Also, it is observed that as the depth of cut and feed rate increase, the feed force increases. Notably, at high depths of cut and feed rates, the presence of graphite decreases feed and cutting force for brass-graphite composite, very significantly from that of monolithic brass.

These machinability tests show that the presence of graphite particles in copper alloy matrix significantly improves machinability. The presence of graphite particle was found to decrease both the cutting and feed forces significantly. In addition, at the higher feed rates and depths of cut, the graphite particles reduces the cutting and feed forces to a very great extent. Also, it can be expected that the graphite particles being so soft that the wear rate of tool will be much reduced.

The cutting force and feed force data between the one inch and three inch diameter pieces also reveal an interesting effect. A careful comparison of data in Tables 1 and 2 (one inch) with these of Tables 3 and 4 (three inch) indicate the following

1. In brass, the cutting force values at both depths of cut for one inch ingots are much larger than those of three inch ingots.
2. In brass-graphite composites, the cutting force values at both depths of cut for one and three inch ingots are almost identical.
3. The same trend is noted in feed force values.

Since plumbing components are usually small in size, the brass-graphite composites offer an additional advantage over brass in their machinability at these small diameters.

Drilling Test :

Samples for drilling tests were cast using an induction furnace. To observe the effect of the distribution of graphite on machinability, two different stirrers, namely, 60 and 45 degree angle blade, respectively, were used to mix the slurry of melt and graphite. Earlier results showed that 60 degree angle blade stirrer improves the distribution of graphite particles in the matrix as well as recovery. For drilling machinability evaluation, three copper alloys were used, namely, a standard yellow brass (C85500 or Cu60-Zn40), yellow brass containing 1.5wt% graphite and 2 wt% Ti, and C90300 containing 1.5wt% graphite and 2 wt% Ti. Machinability tests, namely drillings, were done on 25 mm dia cylindrical ingots along their length at equal spacing of 25mm starting from the bottom, as shown schematically in Fig. 10. A 5.8 mm diameter, 60 degree included angle high speed drill was used at 440rpm under a constant 5 kg force. The depth of drilling was the diameter of cylindrical ingot. Chips from individual locations were collected separately and analysed for total number and total weight. The number of chips per one gram weight was obtained for each location.

Figs. 11 to 14 show the appearance of the drillings taken from the seven different location of each cylindrical ingot. These figures compare the single data of yellow brass with those of the composites; the number of chips varying with drilling locations. It is clearly seen that, in general, the size of chips from the composites are significantly smaller than those of the monolithic alloy, the yellow brass; the size of chips are directly related to the reciprocal of the number of chips per gram. It is also noted that in Fig. 11 that the fairly uniform graphite content of the yellow brass composite at all locations 1 to 7 gave essentially similar chip sizes with some variations at bottom and top locations. In Fig. 12, the C90300 alloy composite gave a fairly uniform chip size throughout locations. With fewer variations in chip size, the sizes of chips are significantly smaller than those of the yellow brass at all locations. The much finer chips near the top are directly related to somewhat a higher content at the top because graphite is a chip breaker similar to lead.

Figs. 11 and 13 data are for a yellow brass-graphite composite and the chip sizes are essentially the same, although in Fig. 11 a 60 degree angle blade stirrer was used to distribute graphite while a 45 degree angle blade stirrer was used in Fig. 13. Similarly, Figs. 12 and 14 can be compared for the C90300 alloy graphite composite. One sees a big difference in chip sizes as reflected in graphite distribution caused by the stirrer blade angle, namely 60 degree angle for Fig. 12 and 45 degree angle for Fig. 14; the 60 degree angle blade produced a good graphite distribution from the bottom to top.

The size of distribution of the chips are given in Table 5 and plotted in Figs. 15 to 18. Figs. 15 to 18 data are for the chip sizes of a yellow brass and yellow brass-graphite composite. The graphite distribution along the ingot height is directly related to chip size which varied in the range of 100 to 300 pieces per gram. Figs. 15 and 16, using 60 degree angle blade stirrer can be compared for Figs. 17 and 18, using 45 degree angle blade stirrer. Here, one sees a big difference in chip size as reflected in graphite distribution caused by the stirrer blade angle, which indicates that 45 degree angle blade stirrer improves the distribution of graphite particles.

3.2.3 Centrifugal casting of Cu alloy containing graphite particle

In centrifugal casting of Cu alloy-graphite composite, the graphite particles are pushed to the inner diameter of the casting while the denser copper melt moves to the outer layer. The distribution of graphite particles depends on many factors, such as the solidification rate of the melt, the mold temperature, particle size, particle density, and the speed and the size of the mold. The aim of this development is to establish the technology of making centrifugal cylindrical casting of copper-graphite alloys with graphite segregating to inner periphery and to find the proper synthesis condition.

A horizontal centrifugal casting machine was used to produce the centrifugal castings. A graphite mold was inserted into a steel die which rotates on a horizontal axis on rollers. The graphite mold was coated with a boron nitride wash which helps in the

removal of the castings. The entire mold was preheated. A suitable pouring cup was designed and fabricated to enable pouring with a minimum amount of turbulence. Alloy C90300 and yellow brass were melted in an induction furnace and graphite powder deagglomerated with aluminum powder was added at about 1100 C using the standard stir cast technology. Ti was added to the melt as a wetting agent. The melt was poured into the mold rotating at a speed of 800 and 1900 rpm. The experimental parameters of these castings are summarized in Table 6.

The microstructure of the castings was characterized and their hardness were determined. Hardness measurements were taken on the cross sections of cylindrical castings, as shown schematically in Fig. 19, using Rockwell hardness tester with 1/16 inch ball. The hardness values were determined in two regions of castings near the front and the rear side of the mold. Samples taken from the different regions were polished and microscopically evaluated. Chemical analysis was carried out on the castings following ASTM 1246 and 663.

3.2.3.1 Microstructure and Chemical Composition

Typical casting and ring section of C90300 and C85500 copper alloys containing graphite are shown in Fig. 20 and it is evident that the experimental conditions used in this study are suitable for casting hollow cylinders of copper alloys containing graphite. In the case of C90300, since its solidification range is very small and the higher viscosity of the alloy slurry due to graphite additions, a proper superheat is required to provide the suitable fluidity.

Centrifugal castings of copper alloys containing graphite are characterized by the presence of two macroscopically distinct graphite free and graphite rich regions, as shown in Fig. 20. Fig. 21 shows the cross section of centrifugally cast copper alloy containing 6.9 and 13 vol% graphite. This figure shows that 13 vol% graphite composite has a relatively larger amount of segregation than 6.9 vol% graphite composite. The segregation

of graphite particles at the inner periphery increases the viscosity, leading to a decreases in the movement of gas bubbles which may be present. As the amount of graphite particle increases, the interaction between the particle and gas bubbles may increase. From the thermodynamic point of view, the particle tends to attach themselves to the gas bubbles to reduce their surface energy. It may be considered that a proper amount of graphite particles is about 6.9 vol% and will reduce the porosity at the inner periphery. In fact, in the tribological point of view, the presence of the porosity at the inner periphery decreases the hardness, leading to an increase in the wear rate under unlubricated operation condition. However, under the lubrication condition, oil can get incorporated in the pores and remain available at the tribosurface, thus reducing friction and wear.

Fig. 22 shows the variation in graphite content with increasing distance from the inner periphery. The observed segregation of graphite particles indicate the movement of much lighter graphite particles towards the inner diameter than the denser molten alloy under the action of strong centrifugal force. Fig. 22(a) shows that the base alloy in the region near the outer diameter contains very little graphite. Fig. 22(b) shows the microstructure of the transition zone which has relatively fewer graphite particles. Fig. 22(c) shows the microstructure of graphite rich region. The elongated cluster of graphite particles may have resulted because the solidification front pushed the particles to the last freezing liquid where these particles become clustered.

Fig. 23 shows the result of chemical analysis. The figures show the distribution of the elements in the outer and the inner periphery of the centrifugal castings of C90300 alloys containing 13 vol% and 6.9 vol% graphite respectively. Fig. 23(a) shows that the graphite in the alloy containing 13 vol% graphite has concentrated at the inner periphery to the extent of 6.31 wt% (total of graphitic carbon and combined carbon) but at the outer periphery it is merely 0.29 wt%. Also, it is noted that there is no significant segregation of tin and zinc between the inner and outer peripheries. The combined carbon analysis indicates that about 0.27 and 0.28 fraction of total carbon is in the form of

combined carbon in the graphite free and rich region, respectively. Fig. 23(b) for the alloy containing 6.9 vol% graphite, shows similarly to Fig. 23(a), that the graphite has concentrated 3.64 wt% at the inner periphery and at the outer periphery to the extent of 0.04 wt%, and while zinc and tin do not segregate radially. The ratio of total carbon to combined carbon in graphite rich region is similar in both the composites. The graphite free region in the alloy containing 6.9 vol% graphite has a lower level of carbon than that for alloy containing 13 vol% graphite. Presence of large amount of graphite in the latter alloy may have contributed to increased viscosity and therefore, possibly a lesser degree of segregation of graphite.

The two castings which have different quantities of graphite particles added to them, initially, namely 13 and 6.9 vol% have their graphitic carbon are 4.54 and 2.65 wt % respectively. In other words, graphite enrichment has occurred in both the cases and this enrichment is expected to be a strong function of rotational speed.

3.2.3.2 Hardness distribution in copper MMC centrifugal castings

Fig. 24 shows the hardness distribution in the radial direction, measured on the longitudinal sections of centrifugal castings of C90300 alloy without graphite cast at 800 rpm. In the monolithic alloy C90300, the hardness is almost uniform at about HRF 80 across the wall thickness. A slightly higher hardness near the outer periphery may be due to the fine structure resulting from rapid cooling caused by mold contact.

Figs. 25 through 27 show the variation of hardness of centrifugal castings containing 3.8, 6.9 and 13 vol.% graphite, as a function of distance from the outer periphery. As expected, with increasing amounts of graphite (a soft material), the overall hardness decreases as one moves through the transition zone to the graphite-enriched inner periphery. The graphite-free regions of the castings have higher hardness values exceeding HRF 75; relatively lower hardness values below HRF 55 are observed in graphite-rich regions. The figures show a transition from graphite free to graphite rich

region in the hardness range from HRF 75 to HRF 55 as one moves from outer periphery towards the inner surface. The transition in hardness distribution takes place over a narrow distance relatively in an alloy containing lower amounts graphite as observed in Fig. 26; in graphite-rich composites the transition is somewhat broader with a larger scatter as seen from Fig. 27. This may be related to several factors, including reagglomeration of graphite particles in the copper melts during hindered movement of particles in the region near the inner periphery, crowded by particles due to action of centrifugal forces. The formation of porosity is normally associated with particles; it is well known that gas bubbles have a strong affinity to particles floating in molten metal. Fig. 27 shows that in the alloy containing 13 vol % graphite, a higher hardness of 90-110 HRF was noted in the outer graphite-free region.

3.2.4 Trobological properties of C90300 alloy containing 13 vol% graphite.

Cylindrically cast C90300 copper alloy samples containing 13 vol% graphite particles were prepared for tribology tests. Pin on disk tests were conducted using a No. 6 Falex machine, in which three pins set in holder were rotated against a disk of gray cast iron. Fig. 28 shows pin set in the holder and disk. The hardness of disk was 74 HRF. The rotational speed was selected to obtain a sliding speed of 1m/s and the applied load was 10, 30, 40, and 60 lb. The pin and disk were weighed before and after each test. the weight loss was measured to 0.1 mg. The torque and temperature were recorded at every 10 seconds to an accuracy of about one percent. Form the measured torque, the values of friction coefficient were calculated based on the applied load and the radius of the rotating pin track. Each test was done for five minutes.

When two material slide together under load, the load deforms the asperities of the contact surface and with friction the temperature rises. In this study, the temperature increase and the friction coefficient were measured. Fig. 29 shows the variation of the weight loss of the pin and disk as a function of load, indicating that as the load increases,

the weight loss of the pin increases, and then at a higher load it decreases. As the load increases, the contact surface is increasingly deformed due to the applied load, and with traction caused by the friction force the deformed asperities are broken and removed as wear particles, leading to weight loss of the pins. It is to be noted that the weight loss of the disk increases with increasing the load and it is less than the pin wear.

5. Conclusions

1. To obtain deagglomerated powder,10 um particle size aluminum powder was mixed intensively with graphite powder in 1:2 weight proportion. Typical microstructure of composites show that premixing with aluminum powder has separated the graphite particles and they are distributed more uniformly in the matrix alloy. The procedure helps to obtain composites with much more uniform distribution of the graphite phase and will significantly decrease the tendency of floatation.

2. The machinability tests show that the graphite particles in copper alloy matrix improves machinability and decrease both the cutting and feed forces significantly. In addition, at the higher feed rates and depths of cut, the graphite particles reduces the cutting and feed forces to a very great extent. Therefore, it can be expected that the graphite particles being so soft that the wear rate of tool will be much reduced.

3. The drilling test showed that the presence of graphite particles reduces the chip size and 60 degree angle blade of stirrer improves the distribution of graphite particles in the matrix which provides the fine chip size.

4. Centrifugal casting study shows that when copper alloys containing graphite are cast centrifugally, the graphite particles selectively distribute themselves in the region near the inner surface of hollow cylinders. The microstructure of the castings reveal that across the thickness, there are graphite free regions and graphite rich regions separated by a distinct transition zone as one moves from the outer to the inner periphery.

5. The chemical analysis reveals a large segregation of most of the graphite near the inner periphery. The hardness test showed that average hardness of the graphite-free regions are similar (above HRF75) but a little higher than that observed in centrifugal castings of the corresponding monolithic matrix alloy. The increase in hardness is attributed primarily to alloying additions for promoting wetting. In the graphite-rich region, the hardness values are relatively lower (below HRF55), and have a wide scatter which reduces with reduced graphite content in the alloy and a higher rotational speed of the mold. A higher scatter has been attributed to graphite agglomeration and some associated porosity.

6. Tribology tests showed that as the applied load increases, the weight loss of pin and disk increases. However, at the higher load, the weight loss of the pin decreases, and that of the disk increases.

6. RECOMMENDATIONS FOR FUTURE WORK

The high melting temperature of copper alloy and the addition of graphite particles increases the viscosity of the copper melt containing graphite particles, leading to difficulties in making a sound casting. The synthesis parameters for centrifugal casting of copper alloy containing graphite particles were determined successfully. On the other hand, the presence of graphite particles in the melt stabilizes the porosity due to a decrease in the surface energy of porosity, and therefore affects the amount of porosity at the inner periphery of castings. Therefore, the amount of the porosity as a function of the rotational speed of the mold and the amount of the graphite particle will be evaluated. Also, the tribological properties of centrifugally cast copper alloy depending on the presence of porosity will be evaluated.

In this year tribology test was done using a cast iron countersurface which contains graphite. In the next year, the counter surface made of steel will be used to evaluate the effect of the graphite on the tribological properties of copper alloy containing graphite particles.

Table 1. Cutting force data for one inch diameter brass and brass-graphite composite castings

	Cutting force (lbf) for brass		Cutting force (lbf) for brass-graphite	
Feed rate (in/rev)	Depth of cut		Depth of cut	
	0.02	0.06	0.02	0.06
0.005	21.7	50.9	11.0	30.5
0.010	33.3	113	16.9	44.7
0.016	53.9	178	29.4	68.5

Table 2. Feed Force data for one inch diameter brass and brass-graphite composite casting

	Feed force (lbf) for brass		Feed force (lbf) for brass-graphite	
Feed rate (in/rev)	Depth of cut		Depth of cut	
	0.02	0.06	0.02	0.06
0.005	7.2	26.7	2.5	12.9
0.010	10.1	43.5	3.2	15.2
0.016	11.5	46.6	3.3	16.4

Table 3. Cutting force data for three inch diameter brass and brass-graphite composite casting

	Cutting force (lbf) for brass		Cutting force (lbf) for brass-graphite	
Feed rate (in/rev)	Depth of cut		Depth of cut	
	0.02	0.06	0.02	0.06
0.005	12.6	41.8	12.0	35.9
0.010	19.0	70.0	18.7	50.0
0.016	33.6	114	28.3	71.1

Table 4. Feed force data for three inch diameter brass and brass-graphite composite casting

	Feed force (lbf) for brass		Feed force (lbf) for brass-graphite	
Feed rate (in/rev)	Depth of cut		Depth of cut	
	0.02	0.06	0.02	0.06
0.005	2.9	18.4	2.7	14.2
0.010	3.4	27.0	3.5	12.7
0.016	4.0	35.0	2.5	18.0

Table 5. The distribution of chips for the various alloy

Alloy	Stirrer blade angle, degree	Number of drilling chips, No/g		Reference
		Minimum	Maximum	
Yellow Brass(C85500) (monolithic)		50	50	Fig. 15
Yellow Brass with 1.5 % graphite and 2% titanium	60	110	280	Fig. 15
C90300 with 1.5 % graphite and 2% titanium	60	150	3100	Fig. 16
Yellow brass 1.5 % graphite and 2% titanium	45	120	310	Fig. 17
C90300 with 1.5 % graphite and 2% titanium	45	225	550	Fig. 18

Table 6. Centrifugal casting parameters of 95mm outside diameter Cu-graphite composite castings.

	C90300	C85500
Rotating speed, rpm	800, 1900	800, 1900
Pouring temperature, C	1100	800
Time of stirring, s	80	80
Ti-Al additive temperature, C	150	150
Mold temperature, C	280-300	280-300
Pouring rate, kg/s	0.5	0.5

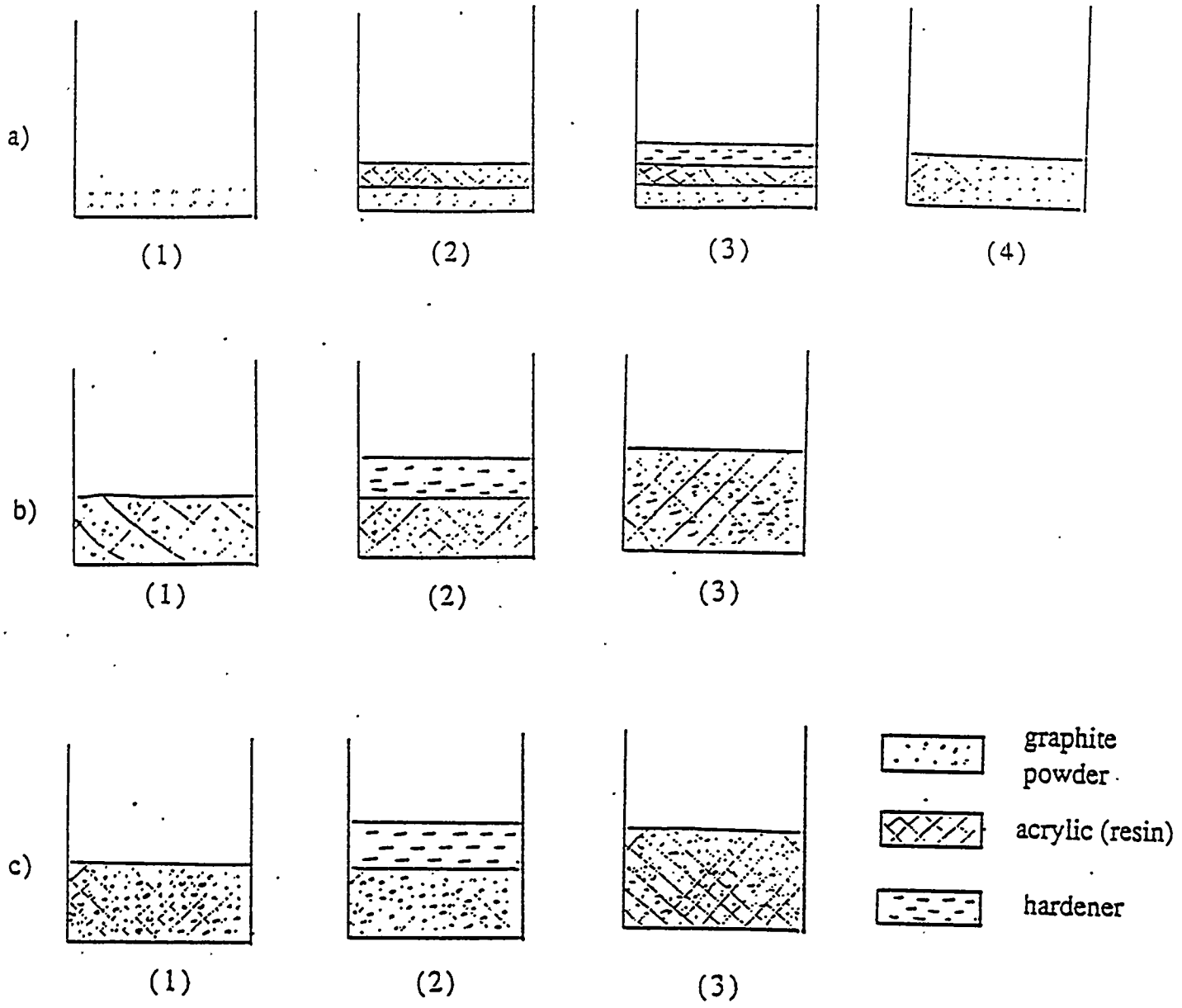

Fig 1. Schematic distribution of different techniques for preparing graphite powder samples for microstructural observation:

a) the "layer by layer" technique

b) sample mixing by blending of two powders

c) mixing by intensive shaking of two powders

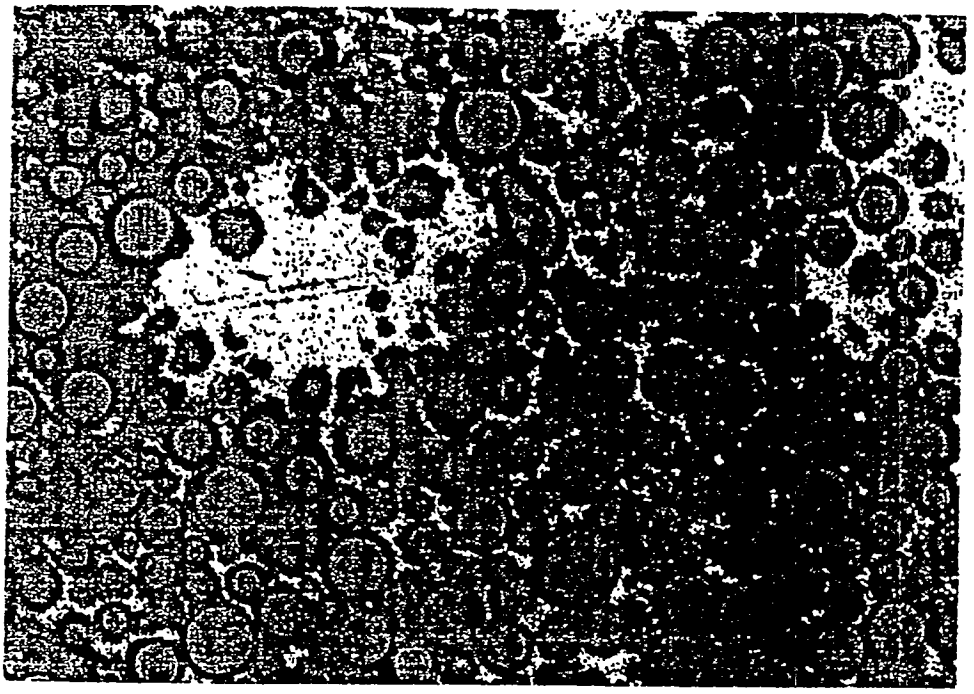

(a)

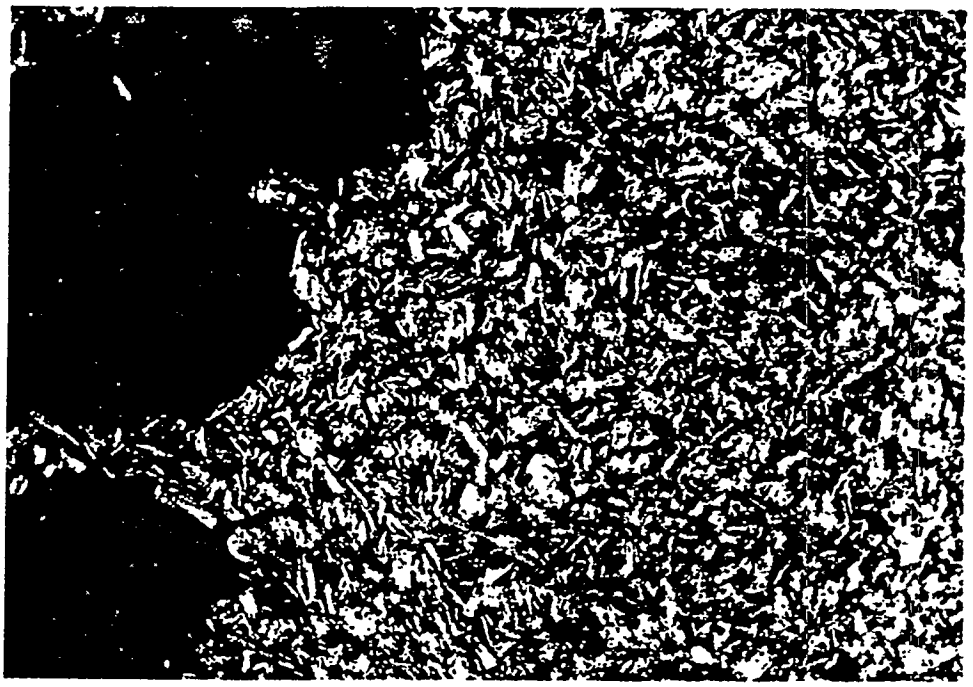

(b)

Fig 2. Microstructure of a mixture of graphite and resin powder obtained by mechanical blending of two powders. a) 50x, b) 500x

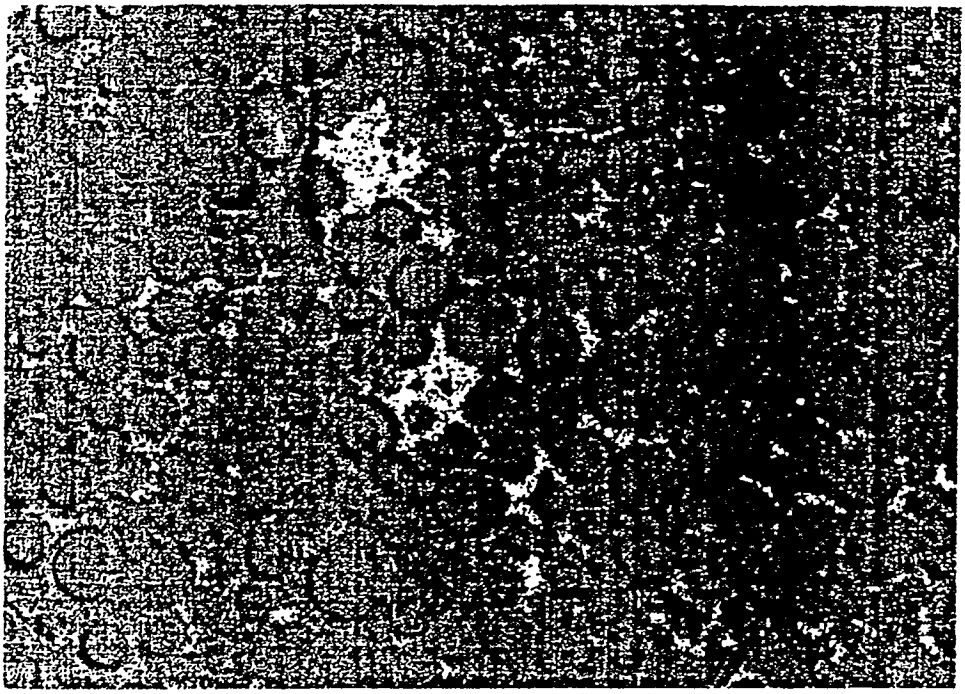

(a)

(b)

Fig 3. Microstructure of a mixture of graphite and resin powders obtained by blending using a layer-by-layer technique. a) 50x, b) 500x

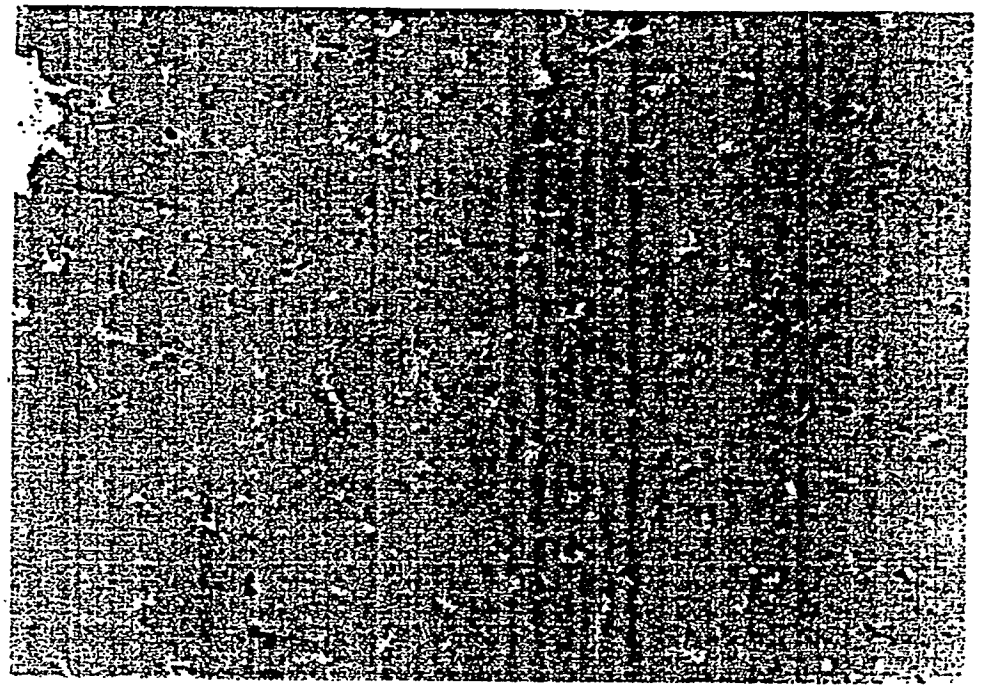

(a)

(b)

Fig 4. Microstructure of a mixture of graphite and resin powders obtained by intensive shaking of two powders. a) 50x, b) 500x

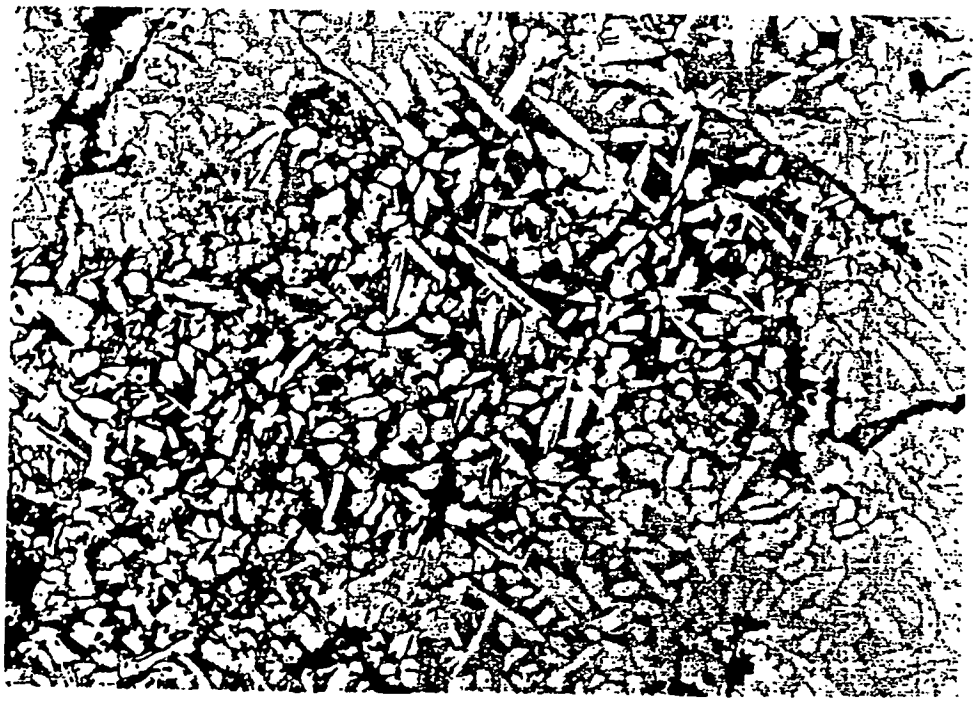

(a)

(b)

Fig 5. Microstructure of a yellow brass-graphite composite casting obtained using a mixture of graphite and aluminum powders. a) 200x. b) 500x

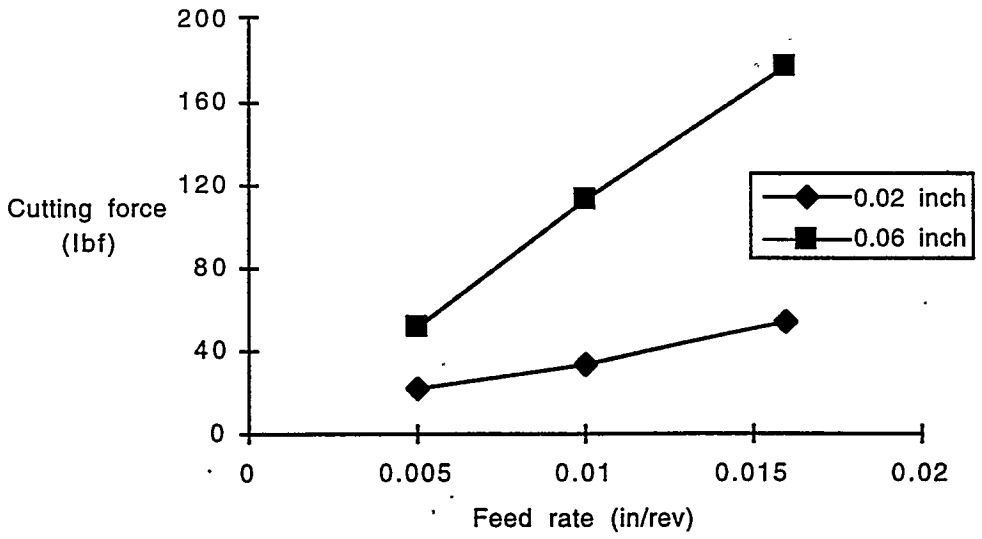

(a)

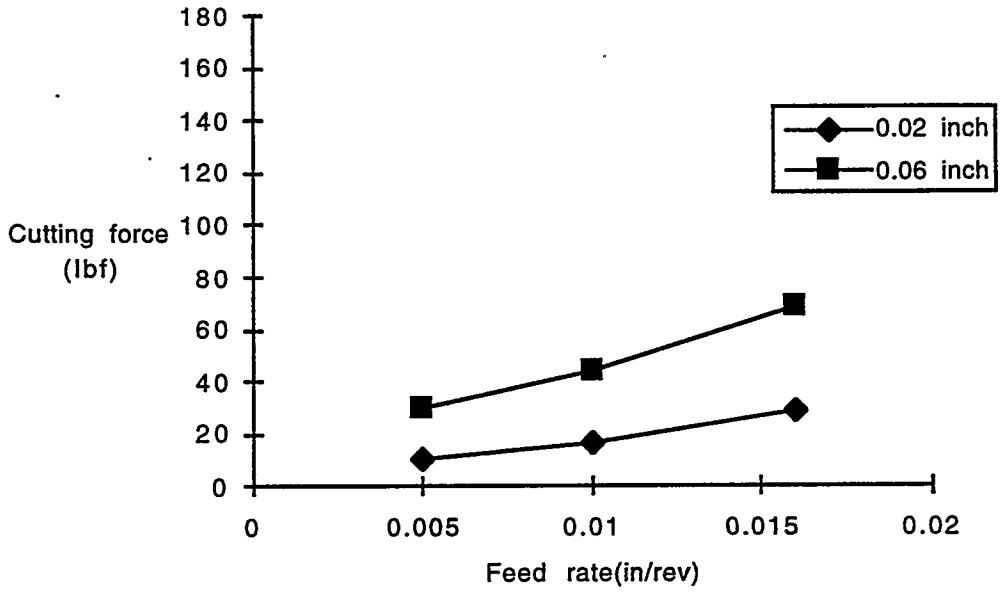

(b)

Fig 6. Cutting force as a function of feed rate and depth of cut in lathe turning of monolithic brass and brass-graphite composite of one inch diameter at 660 sfpm. (a) Monolithic brass, (b) Brass-graphite

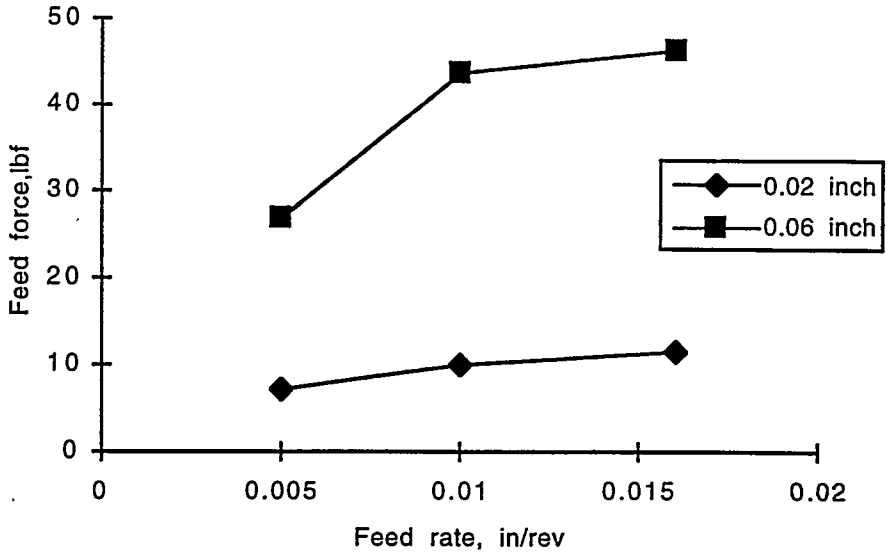

(a)

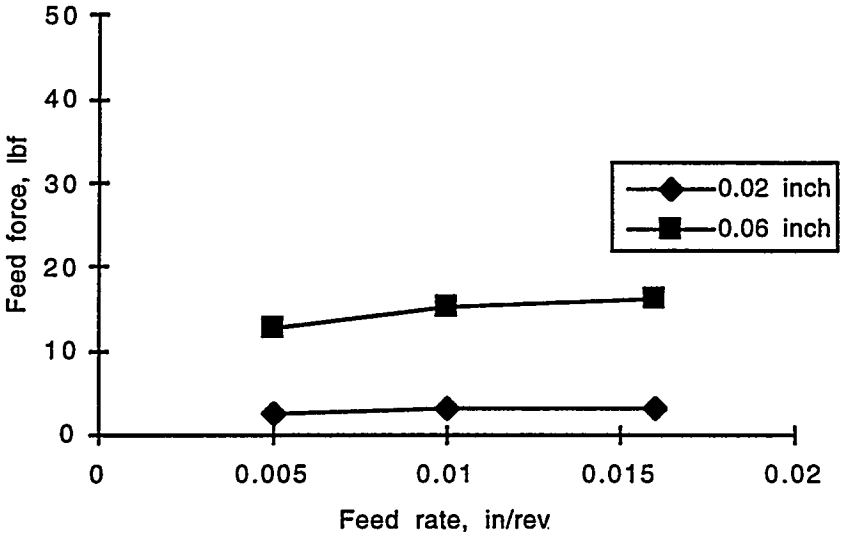

(b)

Fig 7. Feed force as a function of feed rate and depth of cut in lathe turning of monolithic brass and brass-graphite composite of one inch diameter at 660 sfpm. (a) Monolithic brass, (b) Brass-graphite

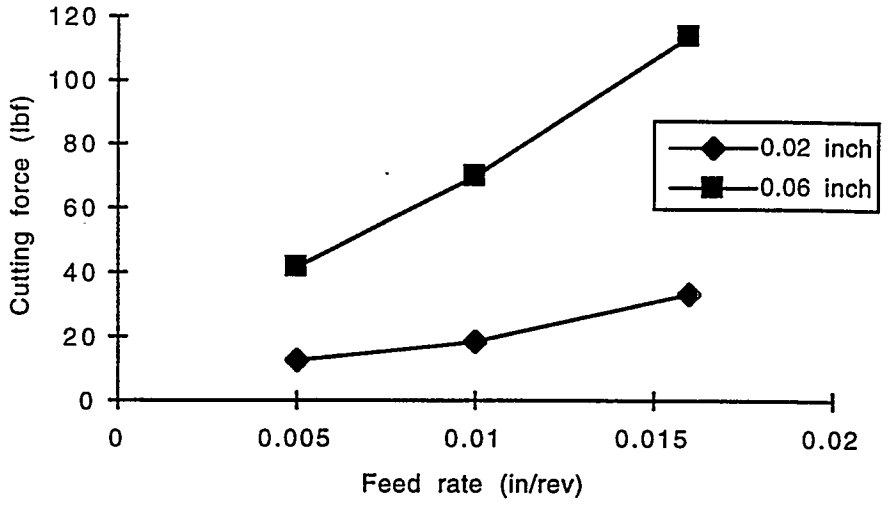

(a)

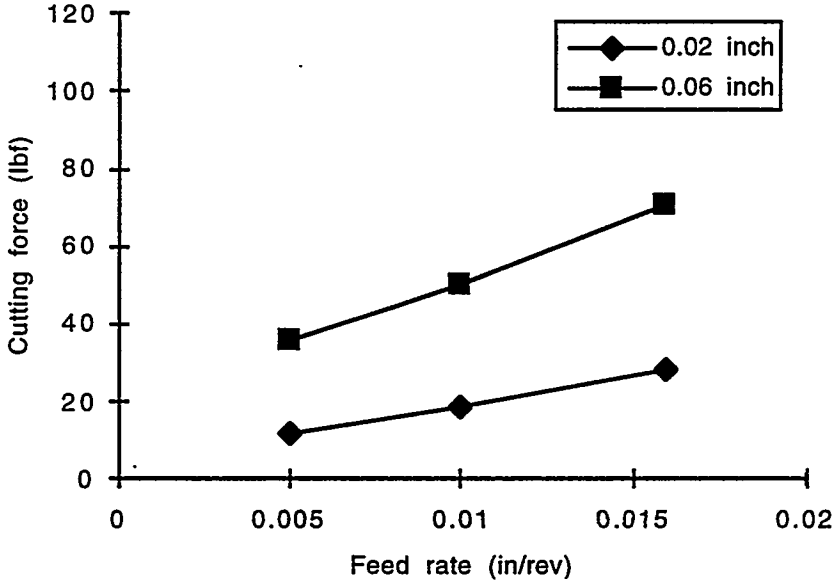

(b)

Fig 8. Cutting force as a function of feed rate and depth of cut in lathe turning of monolithic brass and brass-graphite composite of three diameter at 660 sfpm. (a) Monolithic brass, (b) Brass-graphite

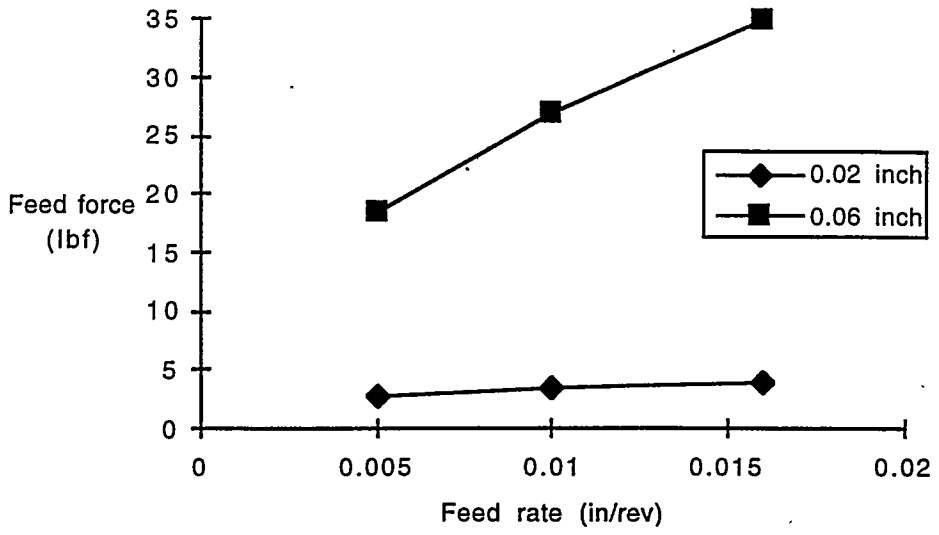

(a)

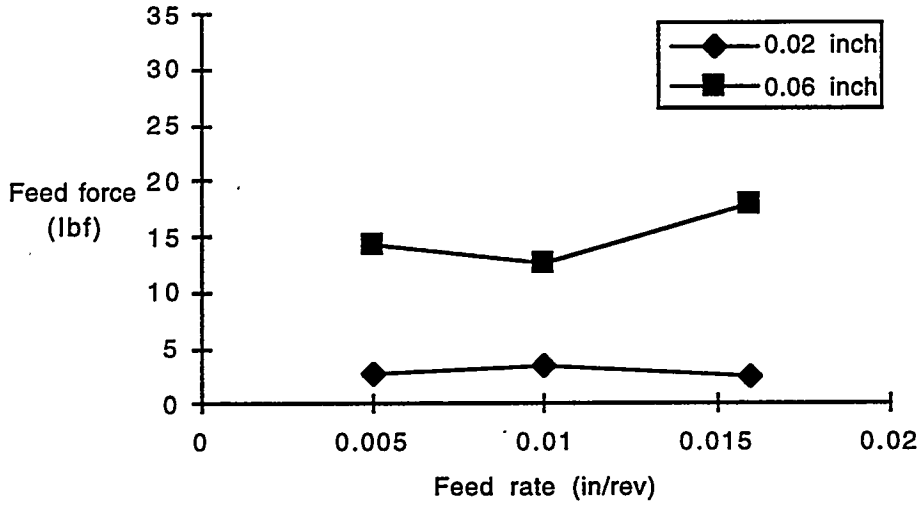

(b)

Fig 9. Feed force as a function of feed rate and depth of cut in lathe turning of monolithic brass and brass-graphite composite of three inch diameter at 660 sfpm. (a) Monolithic brass, (b) Brass-graphite

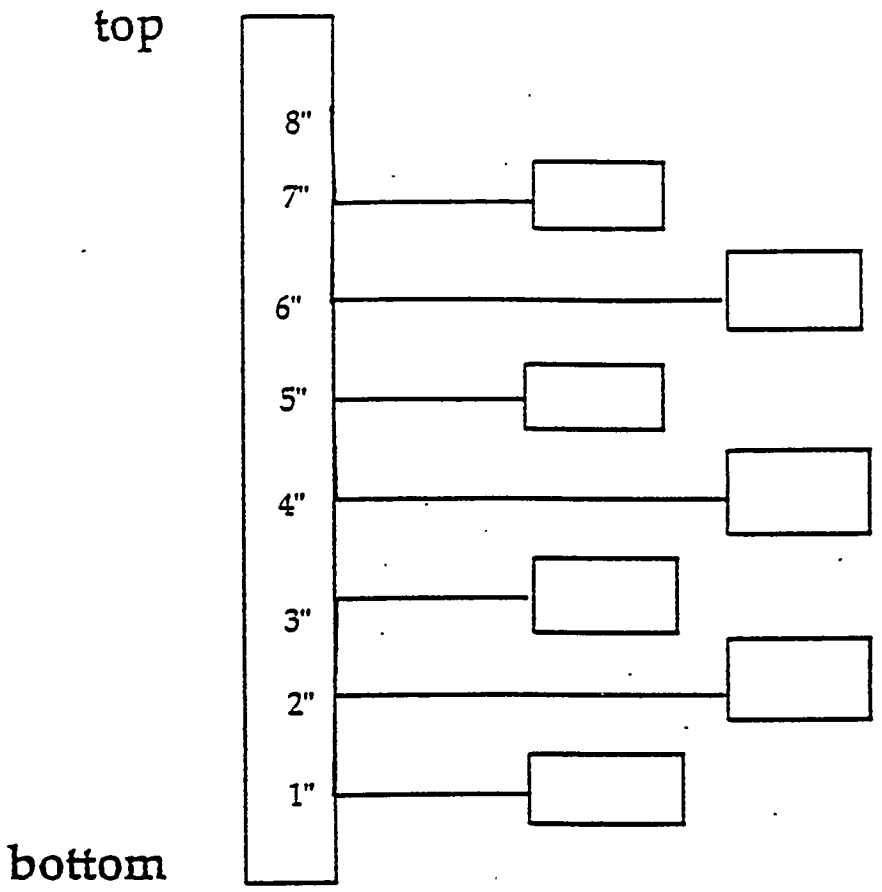

Fig 10. Schematic arrangement of drilling tests on cast brass and other copper alloy-graphite composites. The ingot length 200 mm (8 in.) and diameter 25 mm (1 in.) drilling was made to the centerline of the ingot.

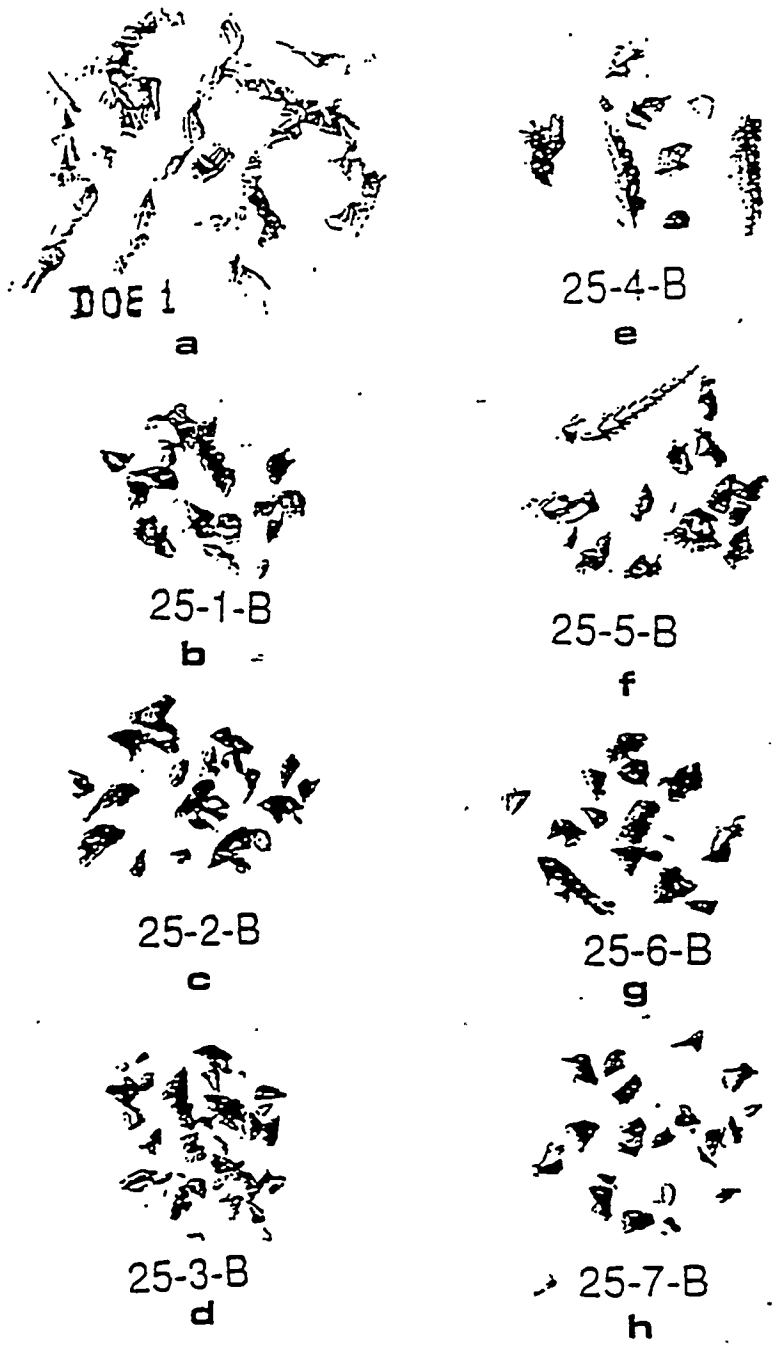

Fig 11. Photographs showing typical drilled chips from cast ingots using a 5.8 mm diameter, 60° angle drill at 440 rpm under an 11 lb (5 kg/f) force. (a) yellow brass, C85500, (b-h) yellow brass with 1.5 wt% graphite and 2% titanium, 60° blade angle of stirrer

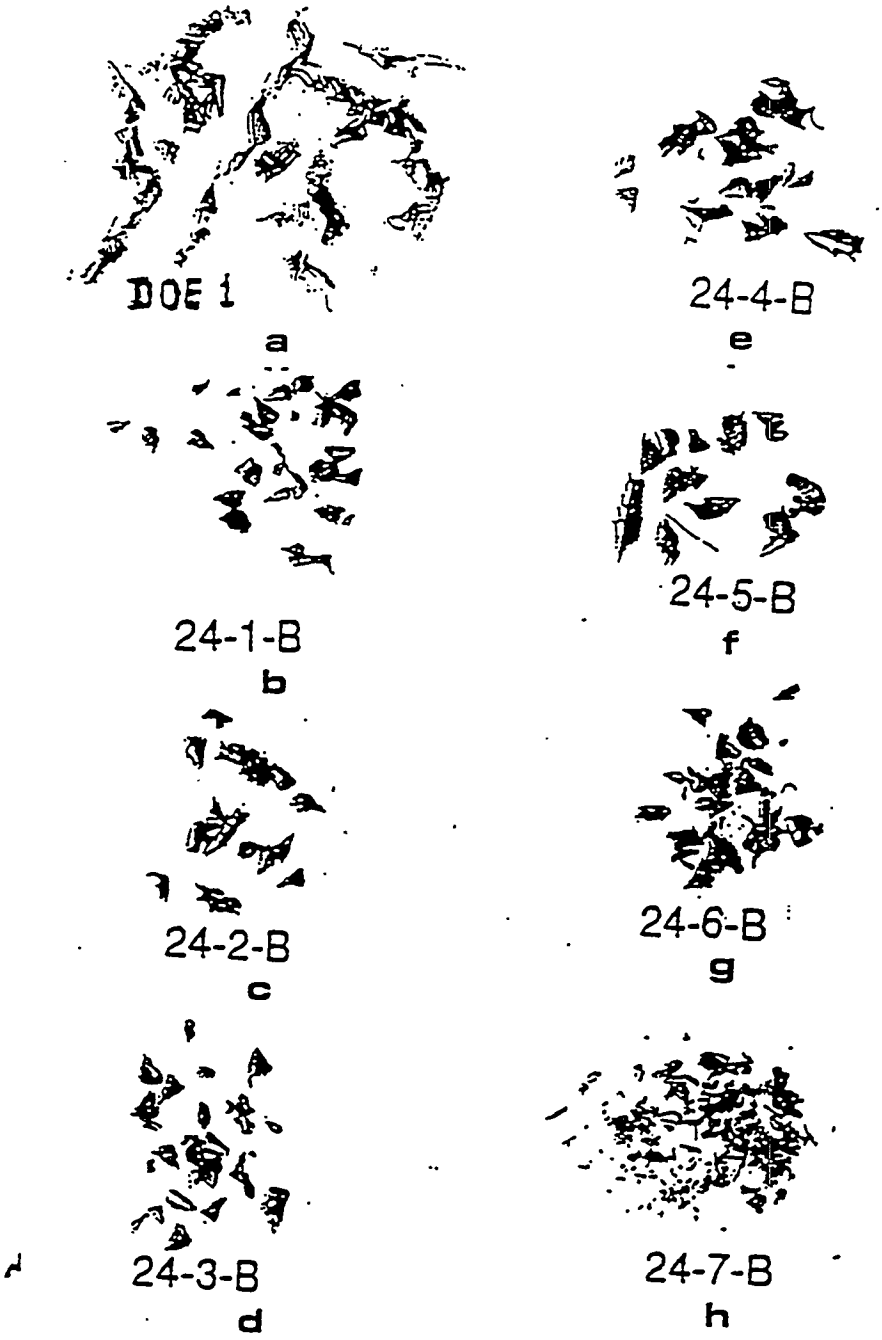

Fig 12. Photographs showing typical drilled chips from cast ingots using a 5.8 mm diameter, 60° angle drill at 440 rpm under an 11 lb (5 kg/f) force. (a) yellow brass, C85500, (b-h) C90300 with 1.5 wt% graphite and 2% titanium, 60° blade angle of stirrer

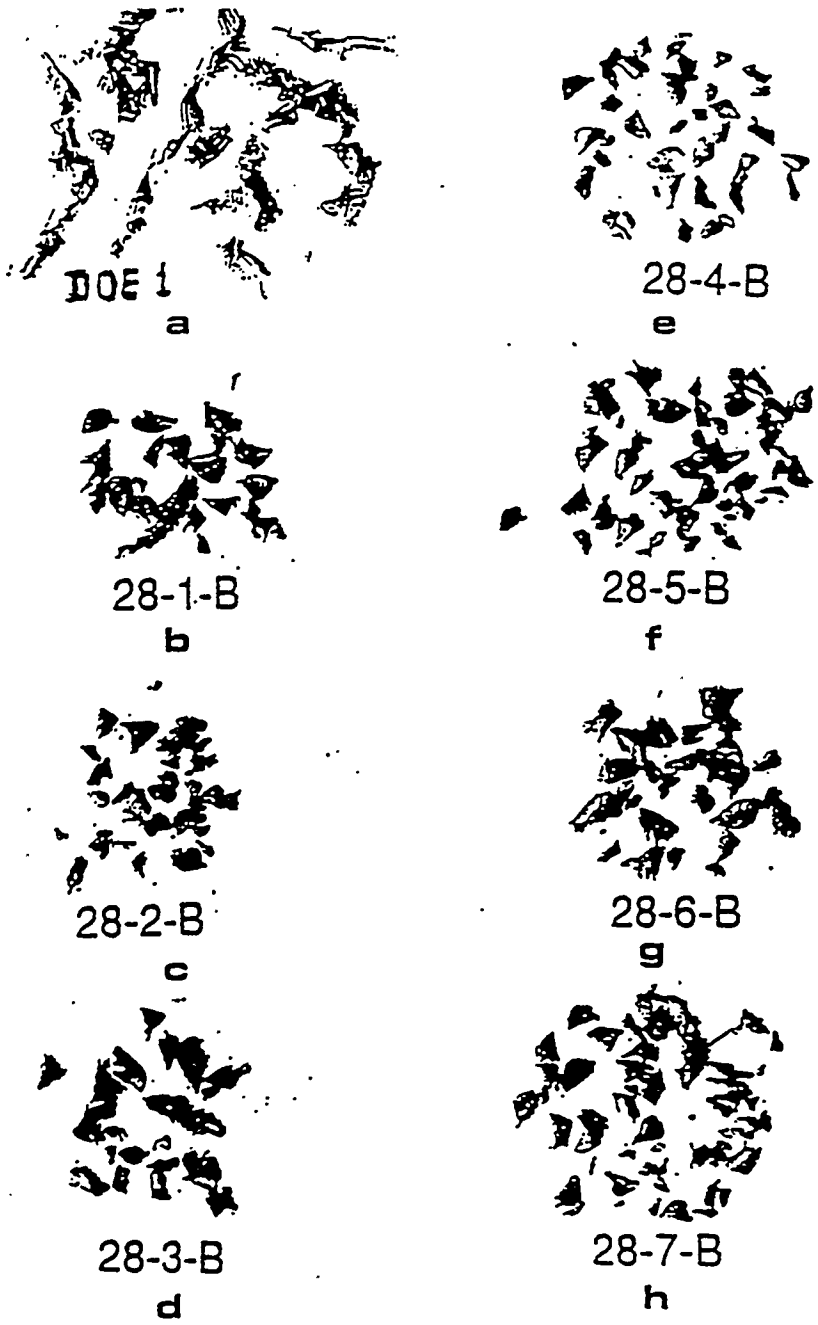

Fig 13. Photographs showing typical drilled chips from cast ingots using a 5.8 mm diameter, 60° angle drill at 440 rpm under an 11 lb (5 kg/f) force. (a) yellow brass, C85500, (b) yellow brass with 1.5 wt% graphite and 2% titanium, 45° blade angle of stirrer

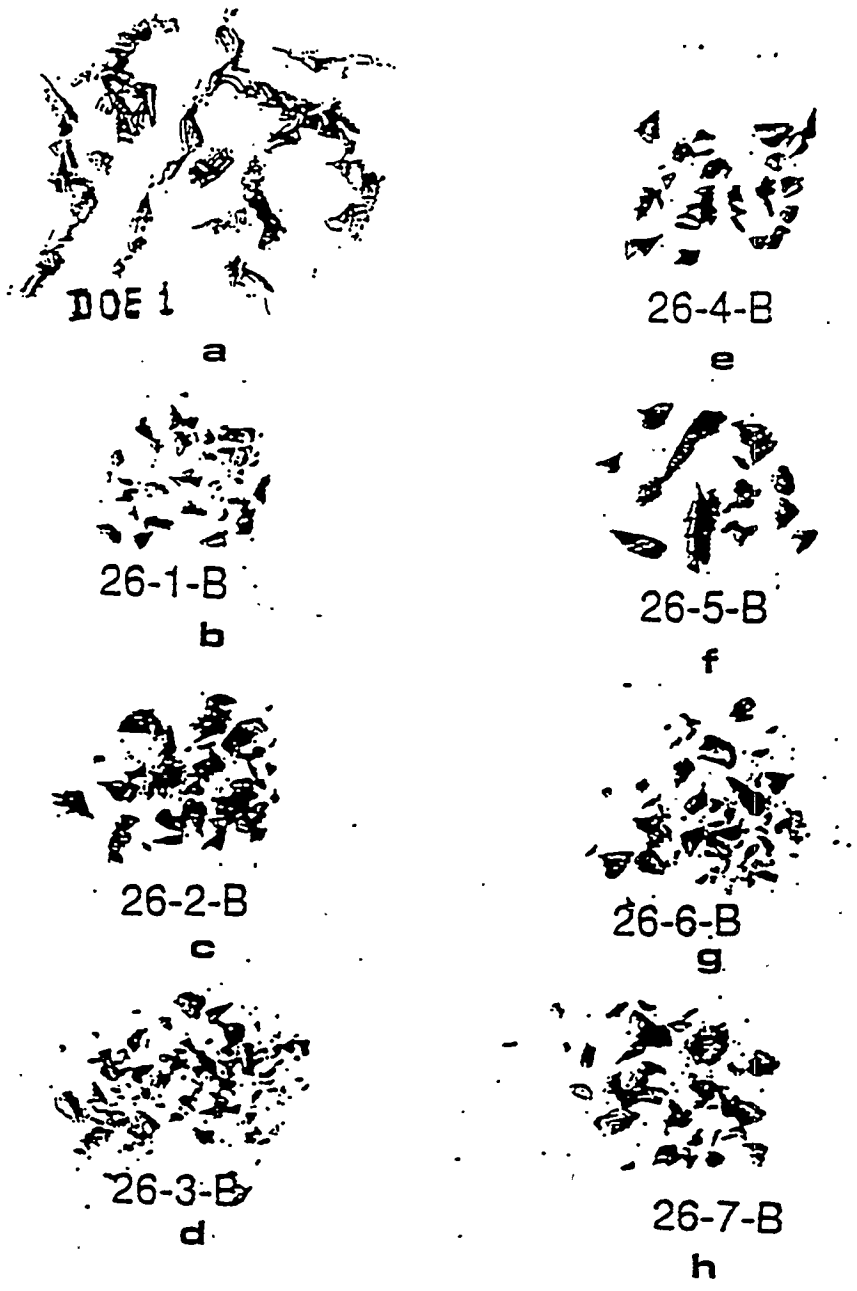

Fig 14. Photographs showing typical drilled chips from cast ingots using a 5.8 mm diameter, 60° angle drill at 440 rpm under an 11 lb (5 kg/f) force. (a) yellow brass, C85500, (b-h) C90300 brass with 1.5 wt% graphite and 2% titanium, 45° blade angle of stirrer

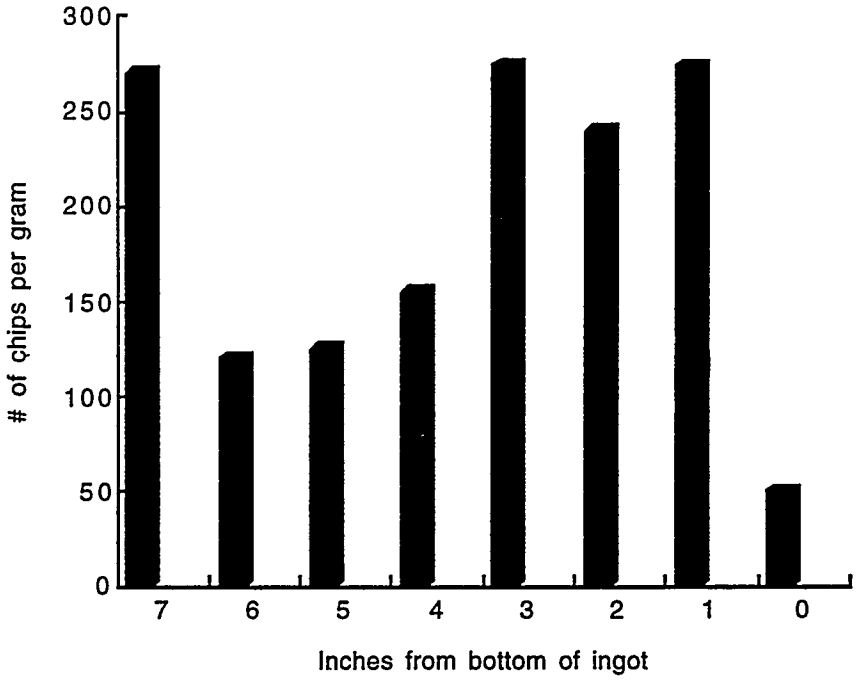

Fig 15. Variation in drilling chip size; monolithic yellow brass. DOE 25 yellow brass-graphite composite, 60° angle blade

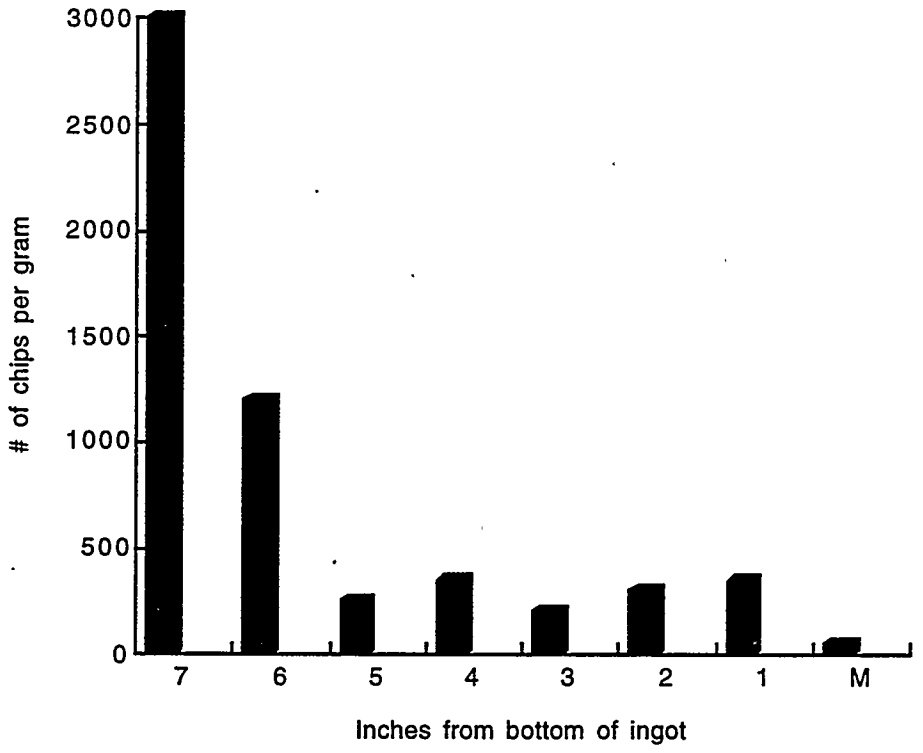

Fig 16. Variation in drilling chip size; monolithic yellow brass. DOE 24 C90300-graphite composite, 60° angle blade. (M: monolithic alloy)

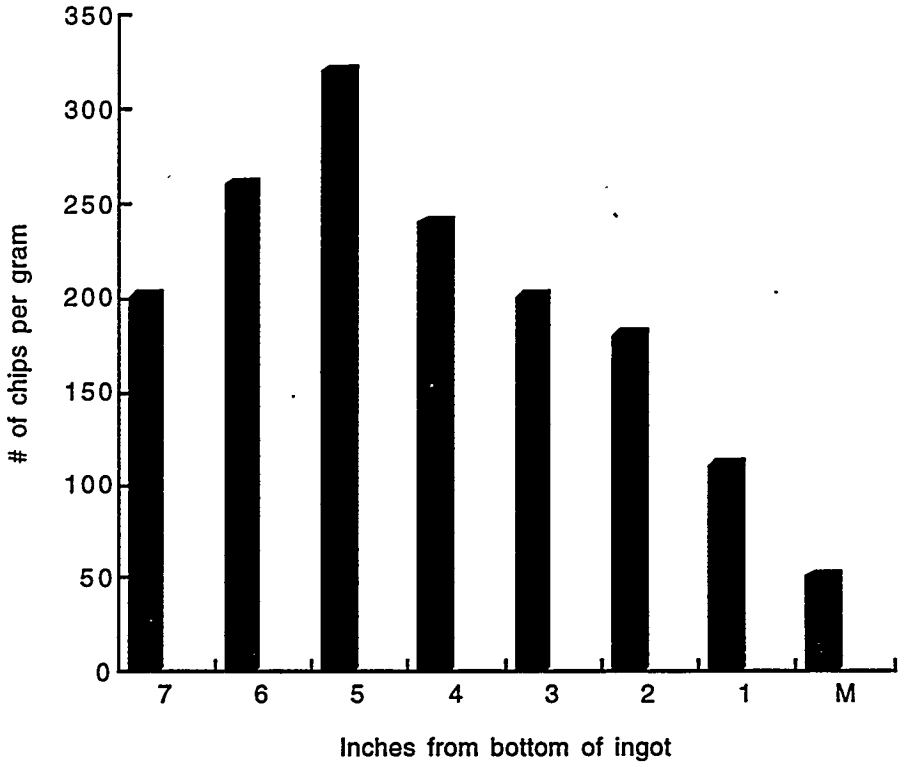

Fig 17. Variation in drilling chip size; monolithic yellow brass. DOE 28 C90300-graphite composite, 45° angle blade

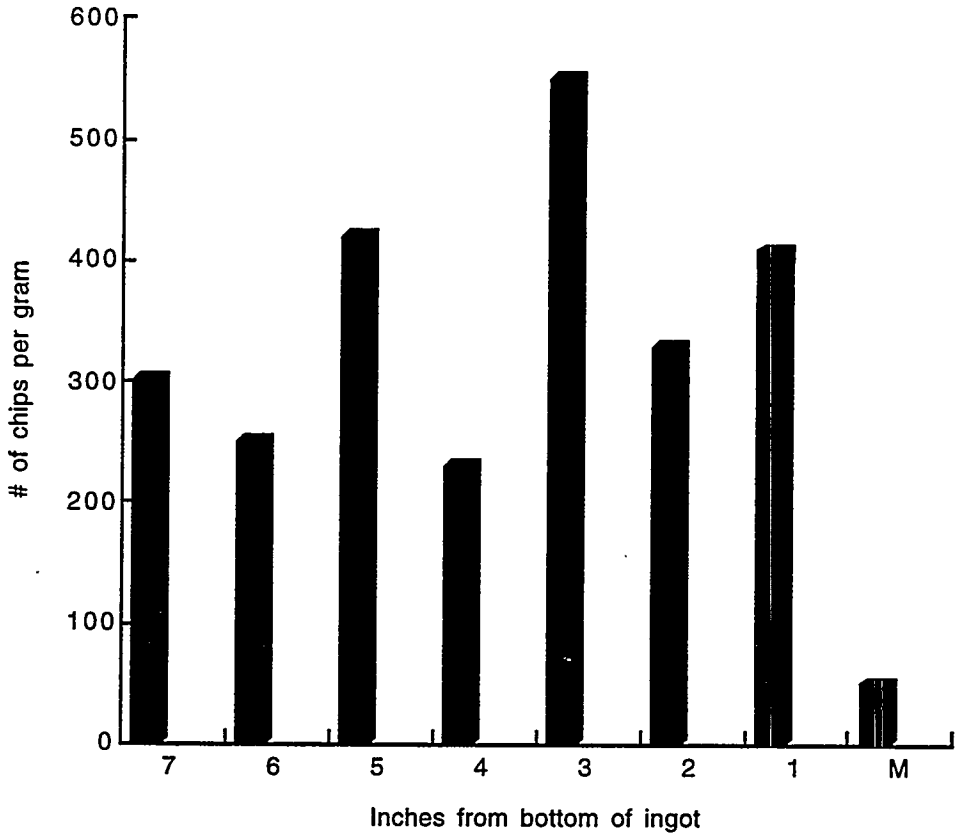

Fig 18. Variation in drilling chip size; monolithic yellow brass. DOE 26 C90300-graphite composite, 45° angle blade

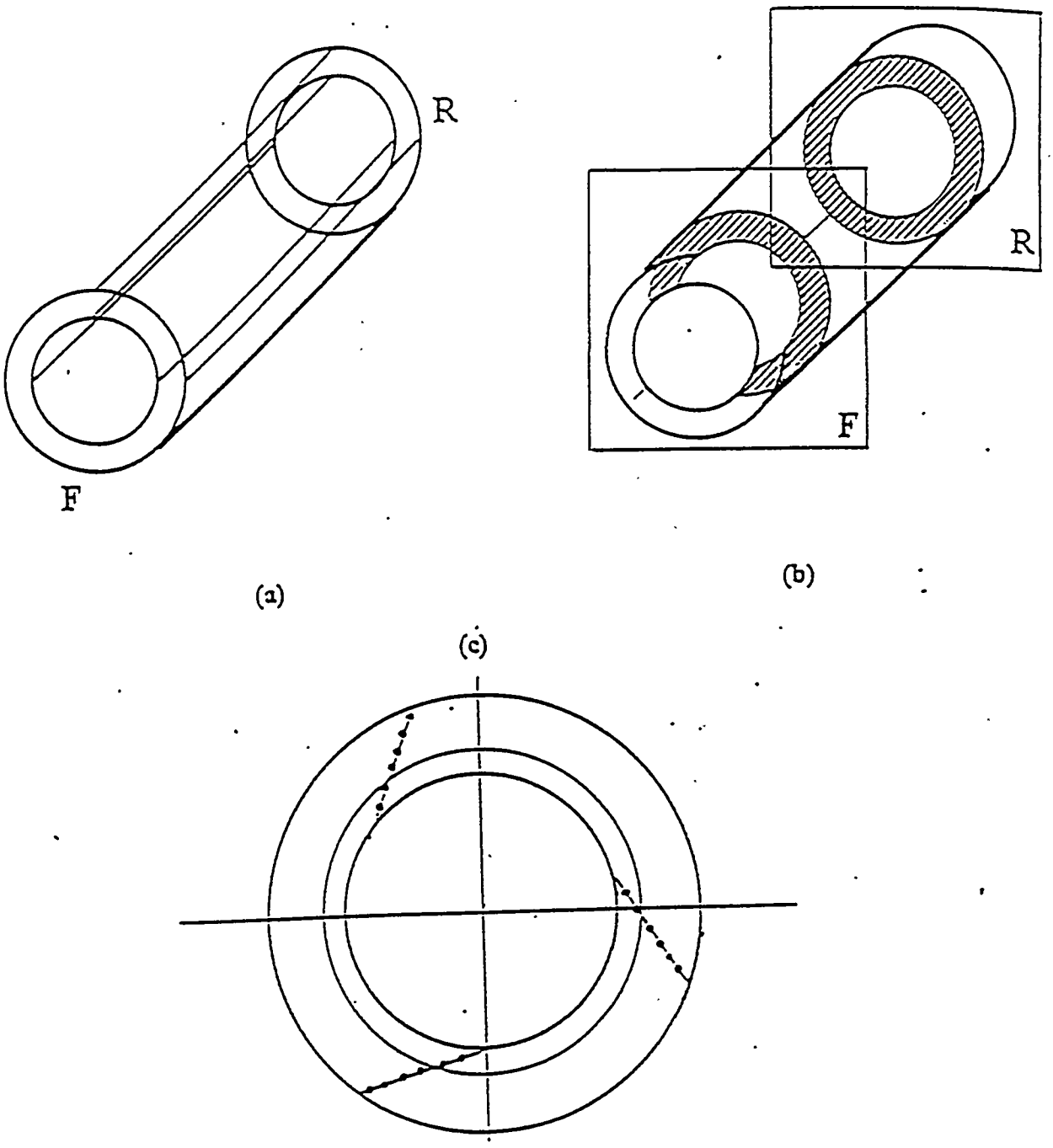

Fig 19. Schematic diagram showing the sites of hardness measurement on the transverse sections (a,b) and longitudinal section (c) centrifugal cast alloys. F: near adjustable runner pot, R: near vertical end wall of centrifugal mold

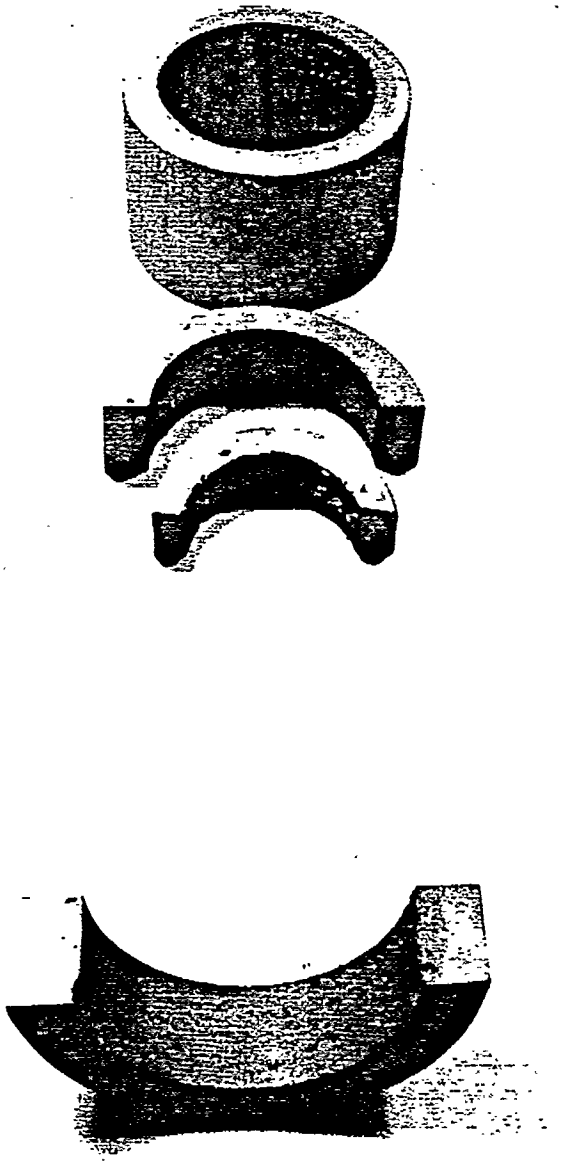

Fig 20. Centrifugal castings of copper alloys containing graphite characterized by the presence of two macroscopically distinct graphite free and graphite rich regions

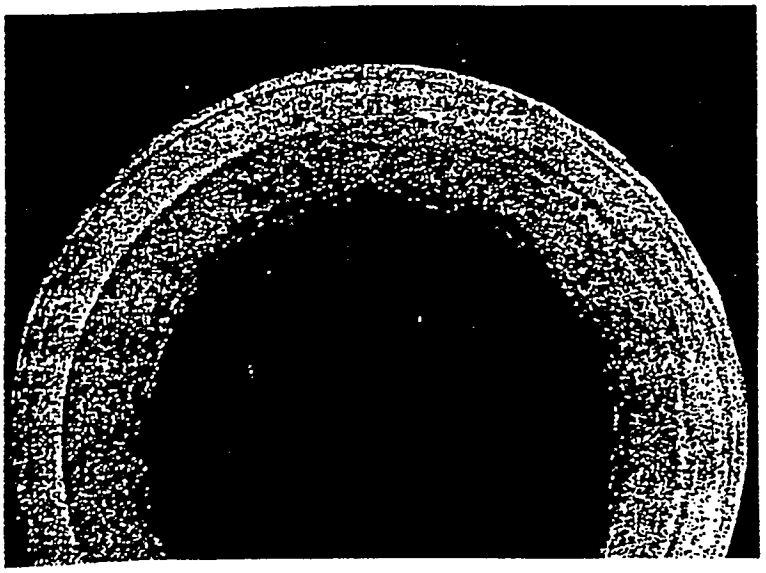

a

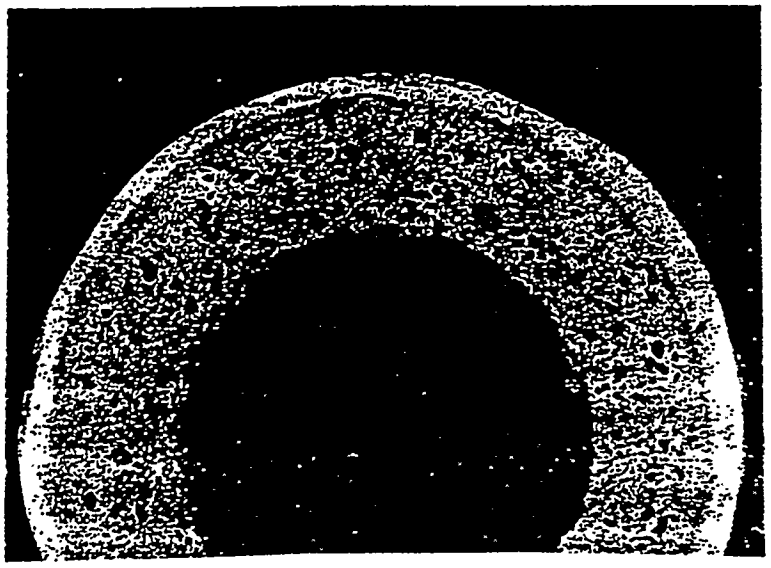

b

Fig 21. Photomacrograph of the cross section of centrifugally cast copper alloy (a) 6.9 vol% Gr (b) 13 vol% Gr

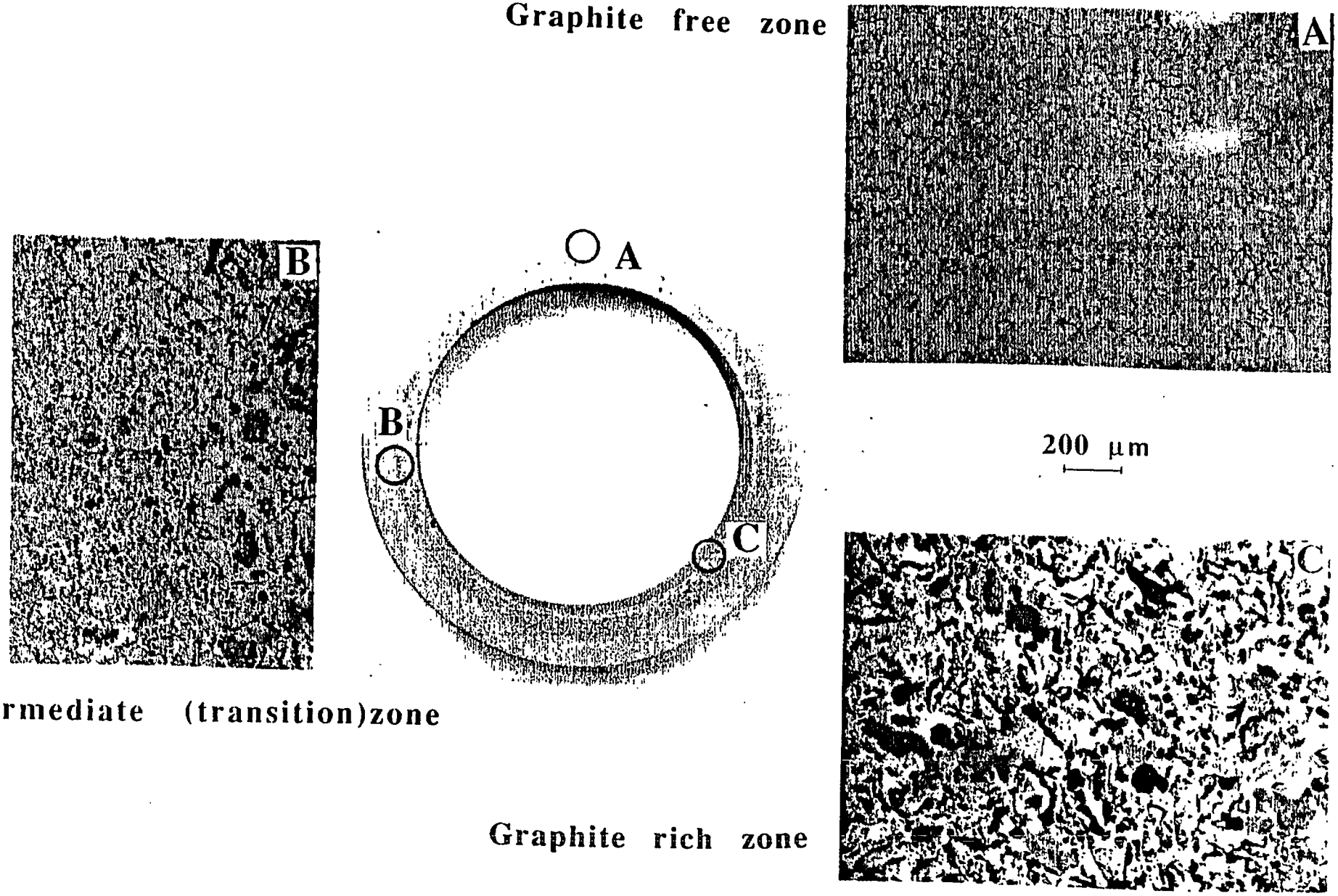

Fig 22. Typical microstructure of copper alloy containing graphite cast by centrifugal casting. (a) graphite free zone, (b) transition zone, (c) graphite rich zone

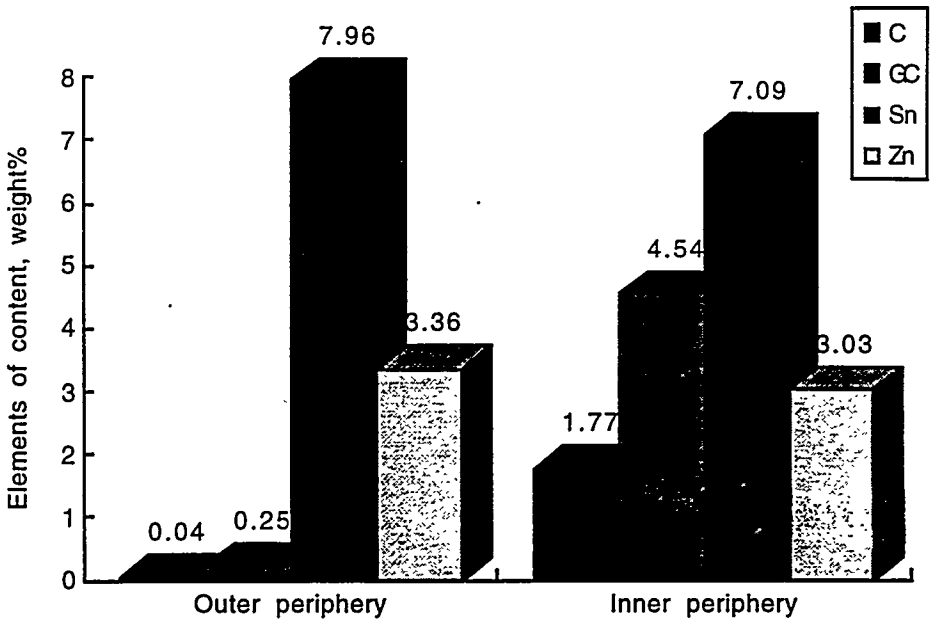

(a)

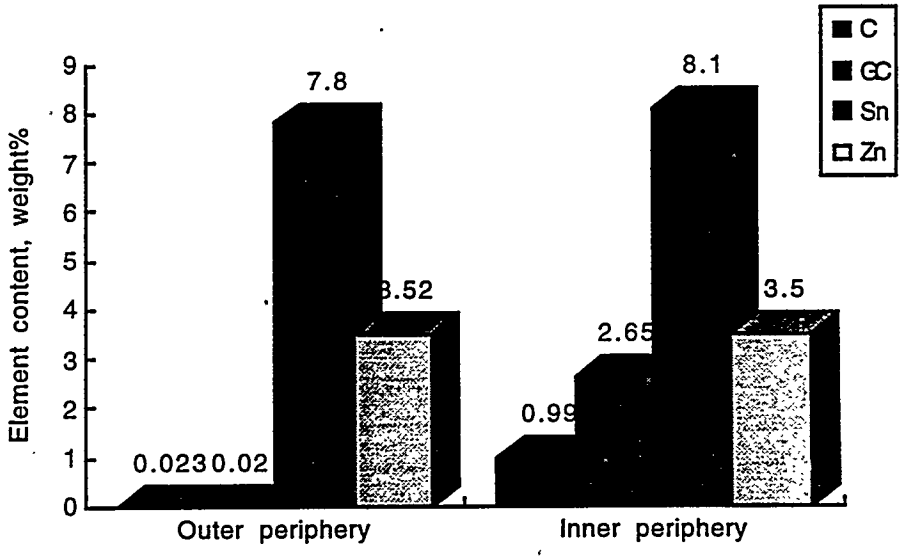

(b)

Fig 23. Distribution of elements in the centrifugal casting (800 rpm) of (a) C90300 alloy containing average 13 vol% graphite, (b) C90300 alloy containing average 6.9 vol% graphite. (C: combined carbon, GC: graphitic carbon)

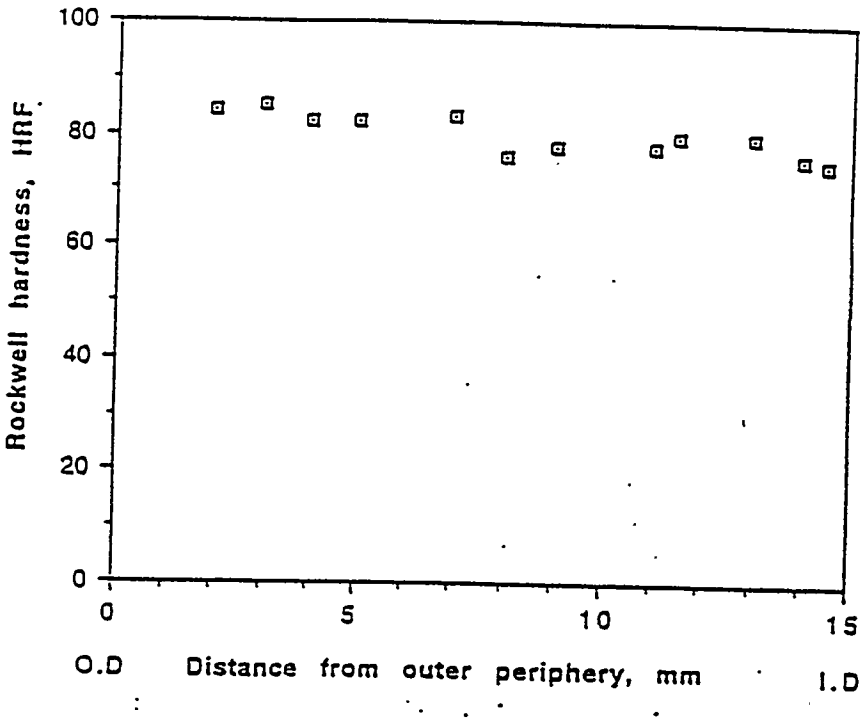

Fig 24. Hardness distribution in the cross section of centrifugal casting of C90300 alloy, cast at 800 rpm

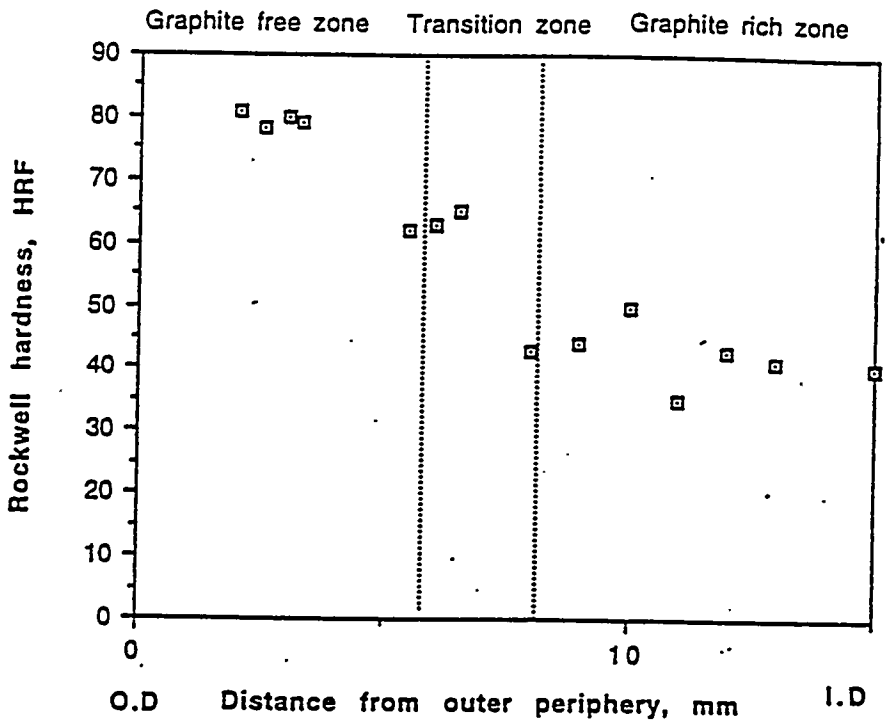

Fig 25. Hardness distribution across the section of centrifugal casting of C90300 alloy containing 3.8 vol% graphite, cast at 800 rpm.

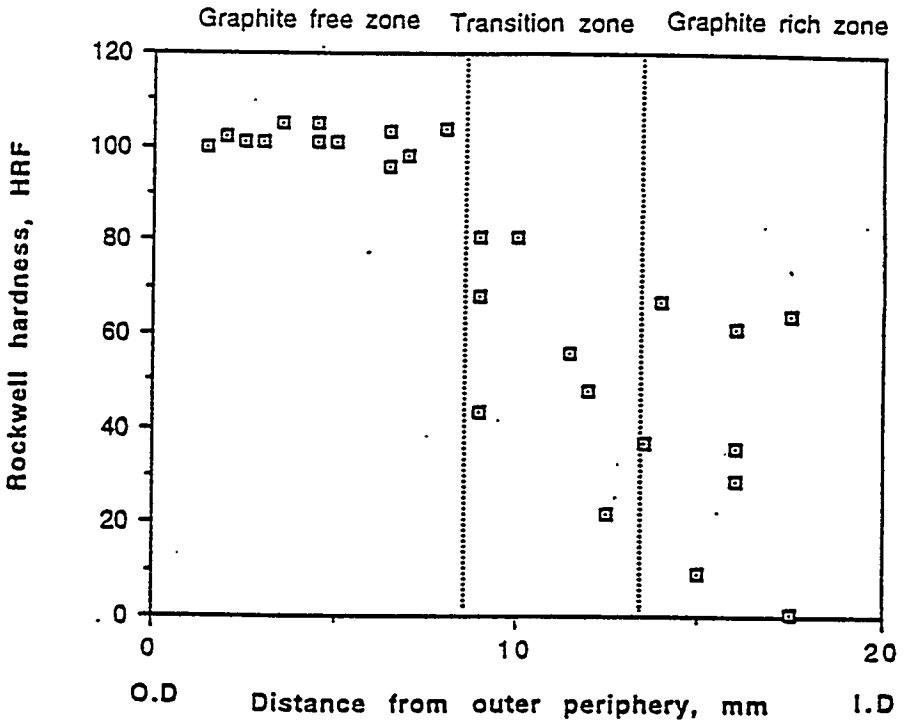

Fig 26. Hardness distribution in the cross section of centrifugal casting of C90300 alloy containing 6.9 vol% graphite, cast at 800 rpm.

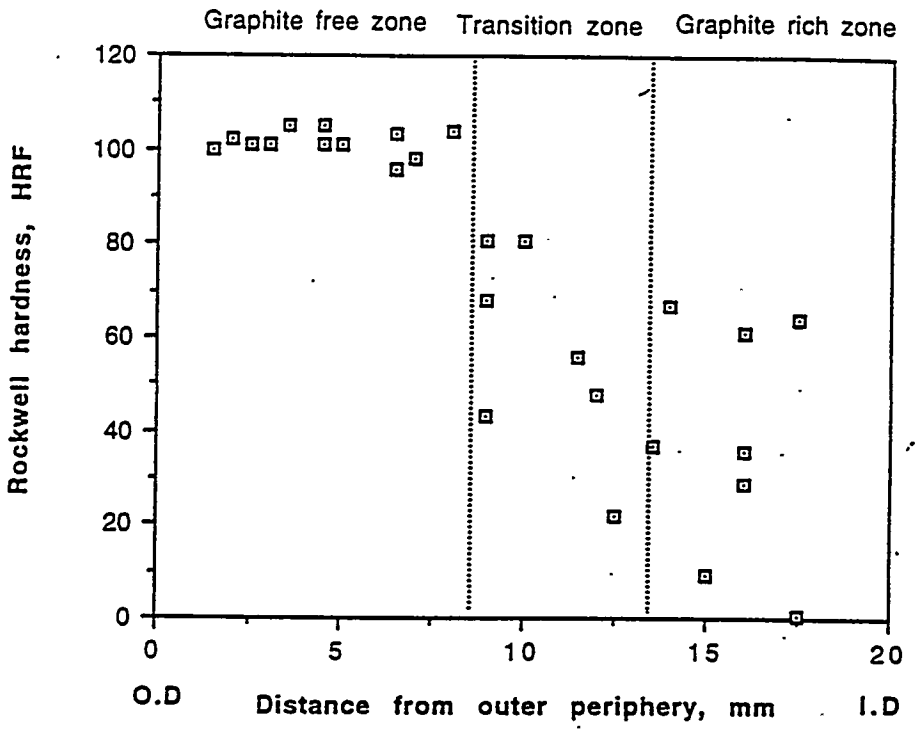

Fig 27. Hardness distribution in the cross section of centrifugal casting of C90300 alloy containing 13.0 vol% graphite, cast at 800 rpm.

Fig 28. The photographs of pin set on the holder and disk.

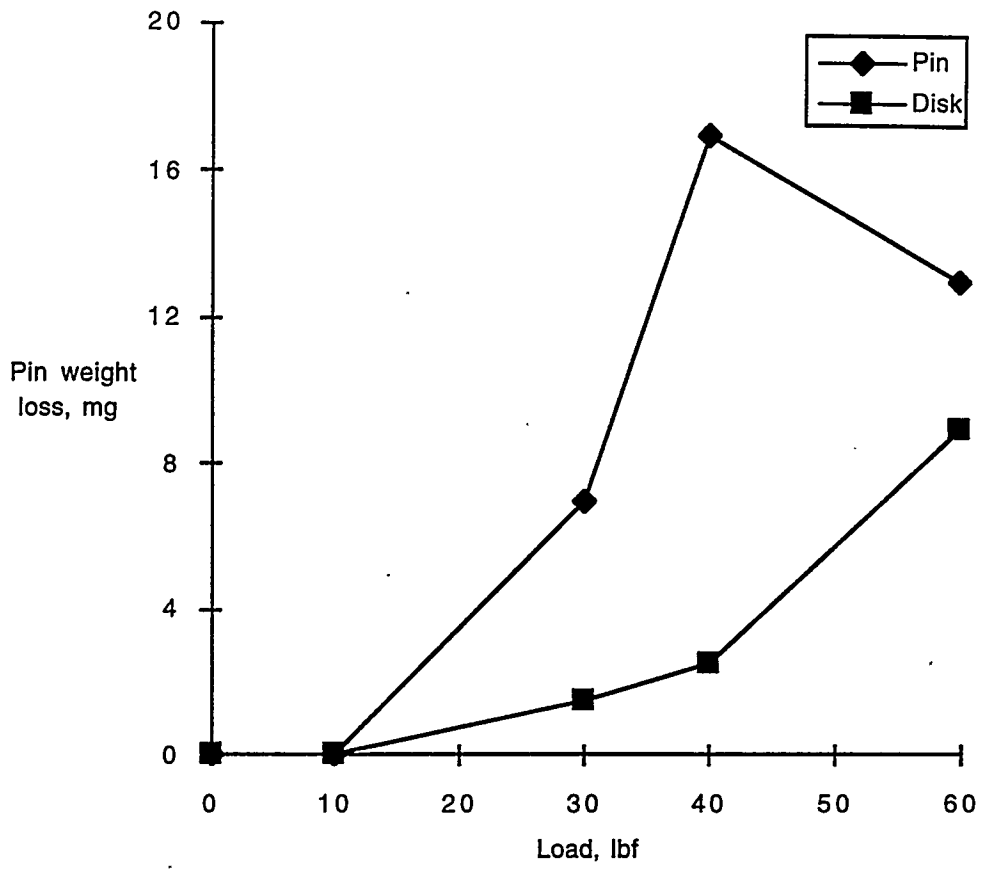

Fig 29. Pin weight loss as a funtion of load